NASA/RSS SMAP Salinity: Version 6.0 Validated Release

Release Notes
Algorithm Theoretical Basis Document (ATBD)
Validation
Data Format Specification
Version History

Thomas Meissner, Frank Wentz, Andrew Manaster, Richard Lindsley, Marty Brewer, Michael Densberger
Remote Sensing Systems, Santa Rosa, CA

With contributions by:
S. Grodsky (UMD), J. Vazquez (JPL), H.-Y. Kao (ESR), D. Levine (GSFC)

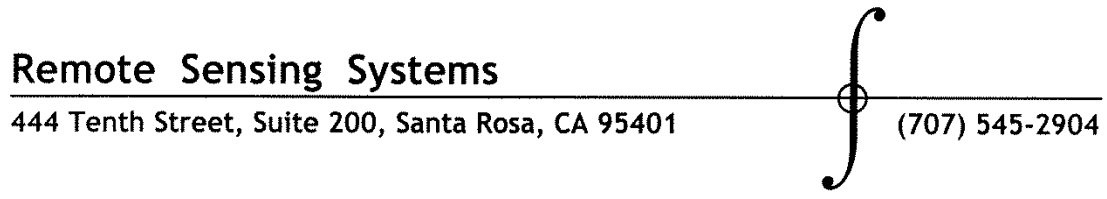

Table of Contents

List of Figures

List of Tables

1 SUMMARY

This document outlines the major steps in the NASA/RSS SMAP Version 6.0 salinity retrieval algorithm and details the data format and specification of the NASA/RSS SMAP Version 6.0 release.

The major achievement in going from Version 2 to Version 3 was consistency with the Aquarius Version 5 end of mission release (Meissner et al. 2017, 2018) and the reduction of spurious temporal and zonal biases over the open ocean that had been observed in the SMAP Version 2 products.

The major change in Version 4 when compared to Version 3 was an improved land correction, which allowed for SMAP salinity retrievals closer to the coast.

The major changes in Version 5.0 from Version 4 were: (1) the addition of formal uncertainty estimates to all salinity retrieval products. (2) Sea-ice flagging and sea-ice side-lobe correction based on direct ingestion of AMSR-2 TB measurements. This is in contrast to Version 4 and earlier versions in which the sea-ice correction was based on an external sea-ice concentration product. The use of AMSR-2 TB measurements in the SMAP Version 5 products onward allows for salinity retrievals closer to the sea-ice edge and aids in the detection of large icebergs near the Antarctic.

The major changes in Version 6.0 from Version 5.0 are: (1) Removal of biases during the first few months of the SMAP mission that are related to the operation of the SMAP radar during that time. (2) Mitigation of biases that depend on the SMAP look angle. (3) Mitigation of salty biases at high Northern latitudes. (4) Revised sun-glint flag.

The standard product of the SMAP Version 6.0 release is the smoothed salinity product with a spatial resolution of approximately 70 km.

2 OVERVIEW OF V6.0 RELEASE

2.1 Release Date

Validated release: 18 January 2024.

2.2 Data Access

- RSS web site: www.remss.com/missions/smap/
- PO.DAAC: https://podaac.jpl.nasa.gov/

Contact: Thomas Meissner, meissner@remss.com.

2.3 Citation and DOI

As a condition of using these data, we require you to use the following citation:

T. Meissner, F. J. Wentz, A. Manaster, R. Lindsley, M. Brewer, M. Densberger, 2024: Remote Sensing Systems SMAP Ocean Surface Salinities [Level 2C, Level 3 Running 8-day, Level 3 Monthly], Version 6.0 validated release. Remote Sensing Systems, Santa Rosa, CA, USA. Available online at www.remss.com/missions/smap, doi: 10.5067/SMP60-xxxxx.

In the doi, the string *xxxxx* is:

1. *2SOCS* for the L2C files.
2. *3SPCS* for the L3 8-day running maps.
3. *3SMCS* for the L3 monthly maps.

Continued production of this data set requires support from NASA. We need you to be sure to cite these data when used in your publications so that we can demonstrate its value to the scientific community. Please include the following statement in the acknowledgement section of your paper:

"SMAP salinity data are produced by Remote Sensing Systems and sponsored by the NASA Ocean Salinity Science Team. They are available at www.remss.com."

2.4 Summary of Updates and Improvements from V2.0 to V3.0

1. Use of Version 4 L1B SMAP RFI filtered antenna temperatures (Piepmeier et al. 2018).

2. Use of the GMF from Aquarius Version 5 Release adapted to SMAP (Meissner et al. 2017, 2018).

   2.1. Use of Liebe et al. (1992) oxygen absorption model.

2.2. Use of surface roughness model from Meissner et al. 2014 with the adjustments specified in Meissner et al. 2018. For deriving the adjustments, the Scripps ARGO analyzed salinity is used as a reference.

2.3. Galactic reflection model based on SMAP fore – aft look analysis (Meissner et al. 2017, 2018).

3. Use of CCMP near real time wind speed and direction as ancillary input.

4. Inclusion of IMERG rain rate. This was used in the atmospheric liquid cloud water correction and for rain flagging.

5. Improved computation of antenna weighted land fraction g_{land}.

6. Improved correction for the intrusion of land radiation from antenna sidelobes.

7. Emissive SMAP antenna:

7.1. The emissivity of the mesh antenna was set to 0.01012 for both V-pol and H-pol polarizations.

7.2. The empirical adjustment to the JPL thermal model was rederived using the Scripps ARGO analyzed salinity field.

8. An error in the computation of the gain-weighted sea ice fraction g_{ice} during 2017 and 2018 in V2.0 was corrected.

9. Antenna Pattern Correction (APC): The spillover, or equivalently the matrix element A_{II} in the APC matrix, was decreased from 1.1080 (V2.0) to 1.0929 (V3).

10. The Level 2C (quality control) flags were updated.

11. The salty biases at low latitudes and the fresh biases at high N latitudes that were observed in the previous release were significantly reduced in V3.0.

2.5 Summary of Updates and Improvements from V3.0 to V4.0

1. Improved land correction: The land tables in V4.0 were derived at 1/8° resolution. In V3.0 the spatial resolution of the land tables resolution had been ½°. The land surface TB that is used in the derivation of the land tables in V4.0 (and subsequent versions) is based on a monthly climatology of SMAP land TB measurements. In V3.0 the land surface TB was based on a land surface emission model.

2. The sea-ice mask in V4.0 was taken from the RSS AMSR-2 sea-ice maps. In V3.0 the sea-ice mask was from NCEP. The threshold for sea-ice exclusion in V4.0 was changed to gice > 0.003. This threshold was gice > 0.001 in V3.0.

3. The sun-glint flag was revised. In V4.0 the sun-glint exclusion was based on sun-glint angle and surface wind speed. The V4.0 sun-glint flag excluded less data than the V3.0 flag did.

4. Starting in Version 4.0, the salinity retrieval algorithm is now run solely on the 0.25° Earth grid using the 40-km spatial resolution Backus Gilbert Optimum Interpolation (OI). The resulting salinity product is called *sss_smap_40km*. From this 40-km product, a smoothed product with a spatial resolution of approximately 70km (called *sss_smap*) is derived using simple next-neighbor averaging. **This smoothed 70-km *sss_smap* is to be regarded as the default (standard) salinity product.** In Version 4 and subsequent versions, both *sss_smap* and *sss_smap_40km* are provided in the same file.

5. An empirical uncertainty estimate, called *sss_smap_uncertainty,* was provided for *sss_smap* in the Level 3 files. This uncertainty was based on comparisons between SMAP and the Scripps ARGO interpolated fields. This also included the sampling error of the Argo data on the scales of the gridded maps, as well as the mapping errors.

2.6 Summary of Updates and Improvements from V4.0 to V5.0

1. The source of the input SMAP RFI filtered TA was consistently: Piepmeier J. et al., 2020. SMAP L1B SMAP L1B Radiometer Half-Orbit Time-Ordered Brightness Temperatures, Version 5. Boulder, Colorado USA. NASA National Snow and Ice Data Center Distributed Active Archive Center. https://doi.org/10.5067/ZHHBN1KQLI20.

2. Formal uncertainty estimates (error bars) were added to all SMAP L2C and L3 salinity retrievals. The empirical uncertainty estimates in the V4.0 L3 products (section 2.5, item 5) were removed.

3. The sea-ice flagging and masking is based on the discriminant analysis of Meissner and Manaster, 2021. It directly ingests 8-day averaged AMSR-2 TB measurements rather than an external, derived ancillary sea-ice concentration. Sea-ice zones that indicate increasing levels of sea-ice contamination in the antenna field of view are identified based on nearest neighbor and next to nearest neighbors of observations that are flagged as sea-ice contaminated. See section 5.3 for further details.

4. A correction for sea-ice contamination in the sidelobes is applied to the measured SMAP TB before salinity is retrieved. See section 5.3 for further details.

5. The *fland* threshold for moderate land contamination was increased from 0.001 (Version 4.0) to 0.005 in Version 5.0.

6. The land correction is not applied if the values of either *gland* or *fland* exceed 0.1, which is defined as strong land contamination (bit 2 of Q/C flag set, section 6).

7. Ancillary atmospheric data, which are required as input into the NASA/RSS SMAP salinity retrieval algorithm to correct for the intervening atmosphere, are now provided by the NCEP 0.25° resolution products. V4.0 and earlier had used the NCEP 1° products for this purpose.

8. The computation of the atmospheric absorption solely uses the NCEP 0.25° cloud water mixing ratio profiles and the L-band cloud water absorption rather than the IMERG rain rate (section 2.4, item 4).

9. The antenna pattern coefficients (APC) (section 4.6) and the ocean target calibration (section 4.7) have been updated to reflect the calibration changes in the V5 SMAP TA (see item 1). In particular, the value of the coefficient A_II was increased from 1.0929 (V3.0, V4.0, prelaunch AP) to 1.1046 in V5.0.

10. The unfiltered TA field was added to the L2C files.

11. The TEC (total electron content) was added as an ancillary field in the L2C files.

12. The aggregate wind speed average was added to the L3 files.

13. The rain filtered L3 products (8-day running and monthly) were included as additional fields into the corresponding netCDF L3 files. In V4.0 and before they had been provided as separate 'rain-filtered' (RF) netCDF files. The ARGO salinity field is no longer provided.

2.7 Summary of Updates and Improvements from V5.0 to V6.0

1. The source of the input SMAP RFI filtered TA is: Piepmeier J. et al., 2023. SMAP L1B SMAP L1B Radiometer Half-Orbit Time-Ordered Brightness Temperatures, Version 6. Boulder, Colorado USA. NASA National Snow and Ice Data Center Distributed Active Archive Center. https://doi.org/10.5067/GWYQTF307Y9Y.

2. During the early months of the SMAP mission (until 08/11/2015) the SMAP radiometer operated in two modes: high-rate (HR) data collection over and close to land and low-rate (LR) data collection over most of the open ocean. This was because, during the operation of the SMAP radar (until July 2015), it was necessary to reduce the data volume that was downlinked from the satellite. Starting 08/11/2015, data have only been collected in HR mode. There is a bias between the HR and LR TA of about 0.25 Kelvin in all polarizations, which is not corrected in the L1B TA processing. This bias results in salty salinity biases near the continental shelf during the early months of the SMAP mission, when both HR and LR collection were done. In the V6.0 SSS release, this bias between HR and LR TA has been manually removed.

3. Small SSS biases that depend on the SMAP look direction have been observed up to and including V5.0. They can be traced back to the reflected galaxy correction. In V6.0 a small adjustment has been made to the reflected galaxy correction, which mitigates these look angle dependent biases.

4. Salty biases at high N latitudes have been observed up to and including V5.0. They can be traced back to the model for the physical temperature of the SMAP mesh antenna. In V6.0 a small adjustment has been made to the physical reflector temperature model, which mitigates these biases.

5. A small revision to the flagging for sun-glint has been made in V6.0.

2.8 Evaluation Version 5.3

The evaluation Version 5.3 is identical to the Version 6.0 validated release with the exception of item 1 in section 2.7. Version 5.3 uses the Version 5 L1B TA as input. The V6 L1B TA uses a lower TA threshold for RFI exclusion. See Piepmeier et al. 2023. Until the full back-processing of V6.0 is complete, the evaluation Version 5.3 can and should be used instead. Version 5.3 has been processed from the beginning of the SMAP mission to the end of 2023.

2.9 Latency

The latency for the FINAL products are:

- L2C: 4-day latency.
- L3 8-day running average: 7-day latency (after the end of the averaging period).
- L3 monthly average: 7-day latency (after the end of the averaging period).

The latency for the NRT (near-real time) L2C files is about 5 hours.

2.10 Spatial Resolution and Spatial Response Function

As was the case in Version 4, the Version 5.0 and Version 6.0 salinity retrieval algorithms are run solely on the 0.25° Earth grid using the 40-km spatial resolution Backus Gilbert (BG) Optimum Interpolation (OI). The resulting salinity product is called *sss_smap_40km*. From this 40-km product, a smoothed product with a spatial resolution of approximately 70km (called *sss_smap*) is derived using simple next-neighbor averaging. That is, the smoothed salinity field S_{smooth} at grid point *(i, j)* is obtained as an equally weighted average over 40-km fields of the 8 adjacent cells and the center cell itself:

$$S_{smooth}(i,j) = \frac{1}{N} \sum_{\substack{k=i-1,i+1 \\ l=j-1,j+1}} S_{40km}(k,l) \tag{1}$$

In (1), *N* is the total number of adjacent cells that go into the averaging. In most instances, *N=9*. However, we apply a quality control (Q/C) and exclude cells that do not pass the Q/C (section 6). In particular, when getting close to the coast, we exclude cells that are contaminated by radiation from land (section 5.1.5).

The smoothed 70-km *sss_smap* is to be regarded as the standard (default) product for scientific applications pertaining to both the open ocean and close to the coast. The smoothed

sss_smap is significantly less noisy than the *sss_smap_40km* products (see Section **Error! Reference source not found.**).

The main reason for retaining the 40-km product *sss_smap_40km* the L2 and L3 files is that it is the actual output of the salinity retrieval algorithm, and we aim to include the results of all major steps in the L2 files. Because of its large noise, the 40-km product is not suitable for most scientific applications. Thus, the L2 and L3 40-km SSS should be considered an *experimental* product for special applications. For example, the 40-km SSS products would potentially be suitable to use when studying areas with large spatial salinity gradients or areas where the surface layer of the ocean experiences freshening under heavy precipitation. In both of these instances, the signal that is to be investigated is significantly larger than the noise from the 40-km product.

Both *sss_smap* and *sss_smap_40km* are provided in the same file.

In V3.0 two separate salinity products were provided. These were resampled at a 40-km (39 x 47 km) elliptical footprint (called "40-km product") and a 75-km circular footprint (called "70-km product"). Doing that turned out to be inadequate for the 70-km product when getting close to land. The BG OI (Appendix A) results in a weighted average of the SMAP observations in the neighborhood of the target cell. Close to land, some of these surrounding cells become contaminated by radiation from the land itself, which is difficult to deal with.

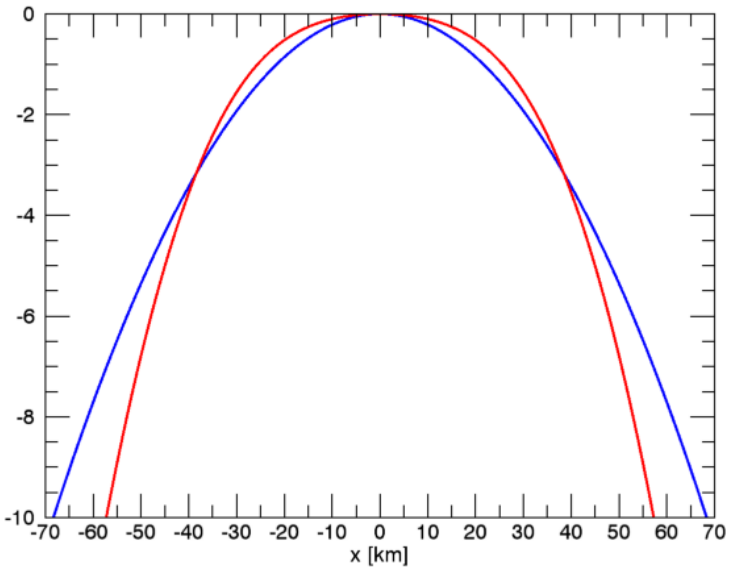

Figure 1: 1-dimensional cross section of spatial response functions (in dB): Blue: Gaussian gain pattern with half-power footprint diameter of 75 km. Red: Average of 3 Gaussian gain patterns whose half-power footprint diameters are 40 km each and who are centered at 0, +25 km, -25 km.

Over the open ocean, the differences between the BG OI in the Version 3 70-km product and the smoothed Version 6 product are small. In Figure 1, we have used a simplified 1-dimensional model to compare the spatial response (gain) of a 75-km 1-dimensional Gaussian footprint (blue) with the one obtained by averaging three 1-dimensional Gaussian 40-km footprints that are centered at -25 km, 0, +25 km (red). If $g_{40km}(x)$ denotes 1-dimensional Gaussian footprint with a half-power (3dB) width of 40km centered at $x = 0$, then the red curve $g_{smooth}(x)$ in Figure 1 is obtained as:

$$g_{smooth}(x) = \frac{1}{3} \cdot \left[g_{40km}(x-25) + g_{40km}(x) + g_{40km}(x+25) \right] \quad (2)$$

This corresponds to the smoothing procedure in equation (1) for the simplified case of 1 spatial dimension. The blue curve in Figure 1 is the 1-dimensional Gaussian footprint $g_{75km}(x)$ with a half-power width of 75 km. The blue and red curves in have approximately the same half-power widths, which is within the mainlobe: $g_{smooth}(x) \approx g_{75km}(x)$. The smoothed *sss_smap* in V6.0 has approximately the same noise reduction as the *70-km sss_smap* in V3.0.

2.11 Known Issues and Missing Data Periods

1. The sea-ice flag and mask based on the AMSR2 TB (section 5.3) is incomplete during a few days. In order to avoid possible contamination from sea-ice, no SMAP salinity retrievals are performed in these cases. Consequently, the L3 products that comprise these dates are produced with a reduced number of observations in the time average. The following dates have been identified:

Table 1: List of dates with incomplete sea-ice flag and mask. No L2 files are produced during these dates. L3 files that comprise these dates have a reduced number of observations in the time average.

year	Month	Day	Day of year
2015	12	3	337
2015	12	4	338
2016	4	15	106
2016	4	16	107
2017	9	27	270
2017	9	28	271
2017	11	25	329
2018	12	16	350

2. There are no CCMP ancillary wind fields for the following days:
   25 – 26 MAY 2017, 22 – 23 OCT 2020.
   No SMAP salinity retrievals are performed during these days. Consequently, the L3 products

that comprise these dates are produced with a reduced number of observations in the time average.

3. The SMAP radiometer was put in safehold mode during Julian days 168 – 206 (17 JUN – 25 JUL) in 2019. No L2C and 8-day L3 files are available during this time period. Monthly L3 files are produced for JUN 2019. No monthly L3 files are produced for JUL 2019.

4. The SMAP radiometer was put in safehold mode during Julian days 218 – 265 (06 AUG – 21 SEP) in 2022. No L2C and 8-day L3 files are available during this time period. No monthly L3 files are produced for AUG – SEP 2022.

5. Undetected RFI is suspected to occur near Japan/China/Taiwan during certain time periods resulting in fresh biases.

6. Undetected RFI is suspected to occur in some areas in the Arabian Sea during certain time periods resulting in fresh biases.

7. Undetected RFI is suspected to occur in some areas in the Mediterranean Sea during certain time periods resulting in fresh biases. The issue has become worse after November 2022 in the area between 15E-35E and 33N-40N.

8. Starting in 2020 an increasing salty bias is observed at high Southern latitudes (around 60S). Possible causes are: (1) A change in the emissivity of the SMAP antenna. (2) A degradation of accuracy of the CCMP ancillary wind speed in the Southern Ocean due to the loss of WindSat as major input source to CCMP.

3 LEVEL 2 PROCESSING

3.1 Input

The RSS SMAP salinity retrieval algorithm ingests RFI filtered antenna temperatures (TA) from the Version 6 SMAP L1B data files (Piepmeier et al., 2023) together with basic spacecraft ephemeris information (S/C location, velocity, and attitude) and time of observation.

3.2 Optimum Interpolation (OI) onto Fixed Earth Grid (L2A)

As a first step, we perform a Backus-Gilbert (BG) type optimum interpolation (OI) (Stogryn 1978, Poe 1990) and resample the L1B TA onto a fixed 0.25° Earth grid at a spatial resolution of approximately 40-km. For details see Appendix A. The resulting gridded TAs are known as Level 2A files. The resampling is done separately for the forward (for) and the backward (aft) looks. This 40-km product (*sss_smap_40km*) maintains the approximate spatial resolution and shape (39 km x 47 km) of the original SMAP L1B swath observations (Piepmeier et al., 2023). The final V6.0 smoothed 70-km *sss_smap* is obtained at each of the 0.25° cells from the *sss_smap_40km* field by averaging the cell with the 8 adjacent 0.25° cells together. **This smoothed V6.0 *sss_smap* field is the default product for science applications**.

3.3 Ancillary Fields (L2B)

The ancillary data sources for the V6.0 Level 2 processing are listed in Table 2. The ancillary fields are space-time interpolated to the location and time of the L2A data in order to create Level 2B files.

Table 2: Ancillary data sources.

Ancillary Input	Data Source
sea surface temperature	Canadian Meteorological Center. 2016 GHRSST Level 4 CMC 0.2deg Global Foundation Sea Surface Temperature Analysis. Version. 3.0. doi: 10.5067/GHCMC-4FM03, http://dx.doi.org/10.5067/GHCMC-4FM03.
sea surface wind speed and direction	CCMP V2.0 near-real time wind speed and direction. http://www.remss.com/measurements/ccmp/. (Mears et al. 2018).
atmospheric profiles for pressure, height, temperature, relative humidity, cloud water mixing ratio	NCEP GDAS ¼ -deg 6-hour. HGT, PRS, TMP, TMP, RH, CLWMR. Available from https://nomads.ncep.noaa.gov/.
IMERG rain rate	Huffman, G. et al., 2019. NASA Global Precipitation Measurement (GPM) Integrated Multi-Satellite Retrievals for GPM (IMERG) Version 6, LATE RUN, 30-minutes, NASA, http://dx.doi.org/10.5067/GPM/IMERG/3B-HH/06.
solar flux	Noon flux values from US Air Force Radio Solar Telescope sites 1415 MHz values. Available from NOAA Space Weather Prediction Center, www.swpc.noaa.gov.

total electron content (TEC)	University of Bern Astronomical Institute (AIUB) Center for Orbit Determination in Europe (CODE) TEC Forecast. Available at http://www.aiub.unibe.ch/download/CODE. The **TEC is not used in the salinity retrieval algorithm**. It is provided as diagnostic information for tracking the calibration of the 3rd Stokes.
sea ice flag and mask	Meissner and Manaster, 2021. The AMSR-2 TB inputs are obtained from RSS AS-ECV www.remss.com/missions/amsr.
land mask	1 km land/water mask from OCEAN DISCIPLINE PROCESSING SYSTEM (ODPS). Based on the World Vector Shoreline (WVS) database and World Data Bank. Courtesy of Fred Patt, Goddard Space Flight Center, frederick.s.patt@nasa.gov.
galactic map	Dinnat, E.; Le Vine, D.; Abraham, S.; Floury, N. Map of Sky Background Brightness Temperature at L-Band. 2018. Available online at https://podaac-tools.jpl.nasa.gov/drive/files/allData/aquarius/L3/mapped/galaxy/2018.
reference salinity (HYCOM) in the ocean target calibration	Hybrid Coordinate Ocean Model, Global Ocean Forecasting System (GOFS) 3.1 output on the GLBy0.08 grid, Top layer salinity. Run by the U.S. Navy. Available at www.hycom.org.

The ancillary TEC maps are not used in in the actual salinity retrieval algorithm. As was the case for the Aquarius salinity retrieval algorithm (Meissner et al. 2017), the Faraday rotation correction in the SMAP salinity retrieval uses the measured 3rd Stokes parameter S3. The ancillary TEC values can be used to check the calibration of S3 by comparing the measured Faraday rotation with the computation based on the ancillary TEC field.

3.4 Salinity Retrieval (L2C)

The SMAP salinity retrieval algorithm is then run on these Level 2B files and produces calibrated SMAP Level 2C surface ocean brightness temperatures (TB) and sea surface salinity (SSS) values.

3.5 Reference Salinity Field

When running the Aquarius and SMAP salinity retrieval algorithms, a reference salinity field is needed for the ocean target calibration (section 4.7). The ocean target calibration ensures that the global average of the Aquarius or SMAP salinity matches the global average of the reference salinity field. For the Aquarius V5 end of mission release, the Scripps ARGO field has been used as reference salinity field in the ocean target calibration. Because of the long latency of the Scripps ARGO field this is not feasible for SMAP, which is an active mission. Therefore, for SMAP the HYCOM field is used as reference salinity field in the ocean target calibration. The globally averaged difference between Scripps ARGO and HYCOM is very small, on the order of 0.02 psu, and therefore the choice between Scripps ARGO and HYCOM is marginal for the ocean target calibration.

When developing the SMAP salinity retrieval algorithm, we also need a reference salinity for the surface roughness correction (section 4.2) and the adjustment to the thermal model for the reflector in the correction for the emissive antenna (section 4.3). The derivation of these corrections does not require a dynamical update. For the SMAP Version 3 through Version 6 re-

leases we use the Scripps ARGO field as reference salinity. In the Version 1 and Version 2 releases, we used the HYCOM SSS fields as a reference salinity. However, this turned out to be inadequate as the HYCOM field has significant temporal and zonal biases when compared to in-situ data. These HYCOM biases are then also visible in the SMAP salinity retrievals. Removing these biases was a major improvement going from Version 2 to Version 3 and using Scripps ARGO instead of HYCOM in the wind emissivity model and the thermal reflector adjustment played a crucial role (see sections 2.4 and **Error! Reference source not found.**).

4 SMAP SALINITY RETRIEVAL ALGORITHM

4.1 Overview and Basic Flow

The basic steps of the SMAP Level 2C salinity retrieval algorithm (Figure 2) have been adapted from the Aquarius Level 2 Version 5.0 (final release) salinity retrieval algorithm and configured for SMAP (Meissner et al. 2017, 2018). The following sections focus on the differences between SMAP Versions 3 through 6 and Aquarius V5.

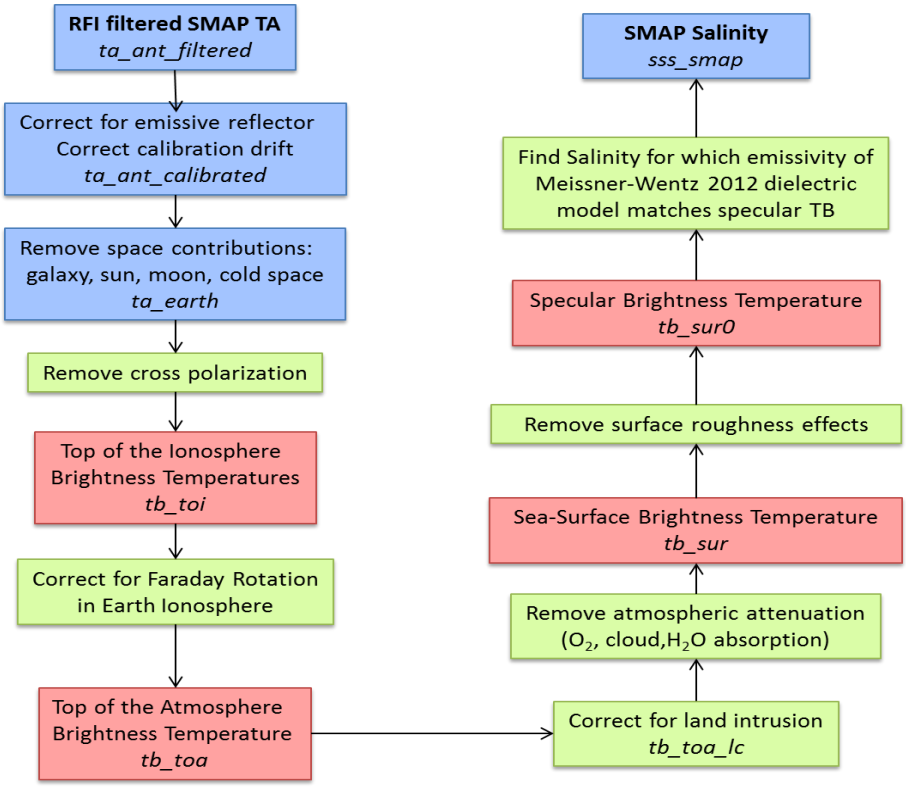

Figure 2: Flow diagram of the SMAP salinity retrieval algorithm.

We use equal channel weights of 1.0 for v-pol and h-pol in the maximum-likelihood estimator (MLE) for the salinity retrieval.

4.2 Surface Roughness Correction

4.2.1 Ancillary Input for Wind Speed and Direction

Due to the loss of the SMAP radar in early July 2015, there are no scatterometer wind speeds available for performing the surface roughness correction. Because of this, the surface roughness correction required to perform the SMAP salinity retrievals uses ancillary wind speeds and directions from the CCMP V2.0 near-real (NRT) time product (Atlas et al. 2011; Mears et al.

2018; www.remss.com/measurements/ccmp/). This Level 4 wind vector product is produced daily at RSS using a Variational Analysis Method (VAM) to blend different satellite wind products and a background wind field. CCMP is produced on a 0.25° x 0.25° Earth grid and has a temporal resolution 6-hours (00Z, 06Z, 12Z, 18Z). The V2.0 NRT CCMP assimilates RSS wind speed and wind direction measurements from the RSS Version 7/8 ocean suite, which includes data from the following sensors: WindSat (until October 2020), SSMIS F16, F17, F18, GMI, and AMSR-2. Because of latency, observations from both RSS ASCAT and RSS' database of quality-controlled moored buoys are not ingested into the V2.0 NRT CCMP processing. The background wind field that is used in the CCMP VAM is the 0.25° field from NCEP GDAS (https://nomads.ncep.noaa.gov/).

4.2.2 Wind Induced Emissivity Model

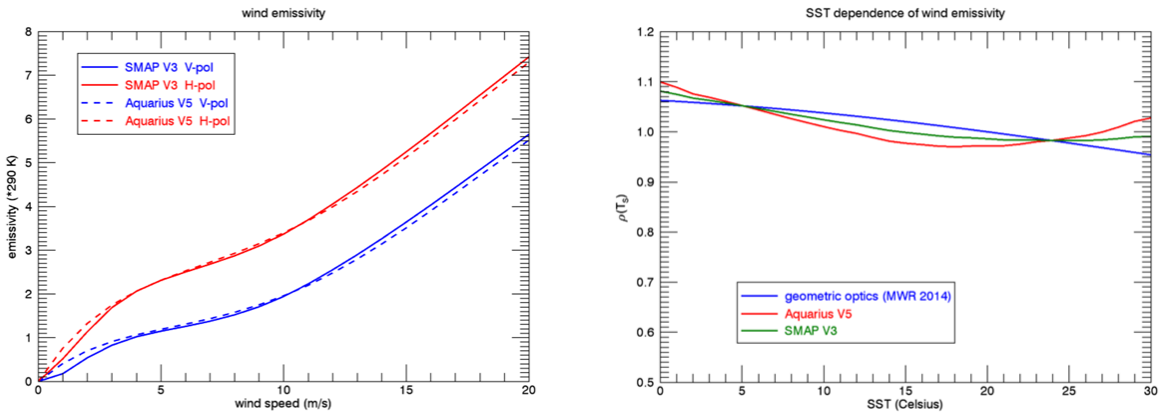

Figure 3: Left: Isotropic (wind-direction independent) part of the wind induced emissivity that is used in the Aquarius Version 5 after interpolating to the SMAP Earth Incidence Angle (dashed lines) and the SMAP Version 3 through Version 6 (full lines) releases. Blue: V-pol. Red: H-pol. The figure shows the 0th harmonic of the wind induced excess emissivity (Meissner et al. 2014, 2017) multiplied by 290 K. Right: SST dependence of the wind induced emissivity for Aquarius horn 2 H-pol. The blue line is the SST dependence from Meissner et al. 2014, which is predicted by the geometric optics model for the wind induced surface emission (Meissner et al. 2012). The red line is the SST dependence used in the Aquarius Version 5 release. The green line is the SST dependence used in the SMAP Version 3 through Version 6 releases (Meissner et al. 2018).

The wind induced emissivity model for the SMAP V3 release onward is based on the wind emissivity model of the Aquarius V5 release after interpolating it to the SMAP Earth incidence angle. There was a small adjustment applied to the Aquarius V5 model function in the SMAP V3 release. This is due to the fact that the CCMP ancillary field is slightly different from the Aquarius HHH wind speed which was used in the Aquarius Version 5 algorithm. Small biases on the order of 0.1 m/s exist between these two ancillary wind fields and are dependent on wind speed as well as SST. Because of the high level of accuracy that is required for retrieving salinity, these biases needed to be considered when deriving the wind induced emissivity model function for SMAP V3 using the method outlined in Meissner et al. 2014. As a consequence of the slightly different ancillary wind speed inputs to the Aquarius Version 5 and SMAP V3 salinity retrieval

algorithms, the geophysical model functions for the wind emissivities also differ slightly. This is most important for the wind speed dependence 0th harmonic coefficient of the wind induced emissivity i.e., the isotropic part. This is shown in the left panel of Figure 3 for SMAP V-pol and H-pol. Small differences are observable at very low and at very high wind speeds. This coincides with the instances where small differences between Aquarius HHH and CCMP wind speeds exist. In addition, we have also found slight differences in the SST dependence $\rho(T_S)$ of the wind induced emissivity, which is shown in the right panel of Figure 3 for the h-pol. The correction term $\rho'(T_S)$ in equation (1) of Meissner et al. 2018, which is empirically determined, is the deviation from the theoretical value predicted by the geometric optics model (Meissner and Wentz 2012; Meissner et al. 2014). This value is reduced by 50% in SMAP Version 3 when compared to Aquarius Version 5. Consequently, the value of $\rho(T_S)$ in SMAP Versions 3 through 6 lies between the theoretical value of the geometrics optics model and the value of Aquarius Version 5.

The derivation of the SMAP V3 wind roughness model uses ARGO Scripps salinity as a reference field to compute the flat surface emission. In the releases prior to Version 3, the HYCOM SSS field was used to derive the surface roughness. This resulted in significant temporal and zonal biases when compared to in-situ data. The main origin of these biases was the HYCOM field.

FORTRAN90 and IDL routines that compute the SMAP V3 wind induced emissivity model function are available together with these release notes at www.remss.com/missions/smap/.

The SMAP V4, V5, and V6 releases use the same wind emissivity model as in V3.

4.3 Correction for Emissive SMAP Antenna

4.3.1 Correction for Emissive SMAP Antenna in V3 – V5

The emissivity of the Aquarius antenna was negligible for all practical purposes. SMAP, however, has a mesh reflector which has an emissivity of about 1%. This is large enough that a correction needs to be applied in the salinity retrieval. If T_A is the antenna temperature before the radiation hits the reflector whose physical temperature is denoted by T_{refl} and whose emissivity is ε_{refl}, then the resulting antenna temperature T_A' that enters the receiver after the reflection is given by:

$$T_A' = (1-\varepsilon_{refl})\cdot T_A + \varepsilon_{refl}\cdot T_{refl} = T_A + \varepsilon_{refl}\cdot(T_{refl} - T_A) \quad (3)$$

In order to perform this emissivity correction (i.e., determine the value of T_A from the measured T_A' according to (3)), it is necessary to know the values of both the reflector emissivity ε_{refl} and its physical temperature T_{refl}.

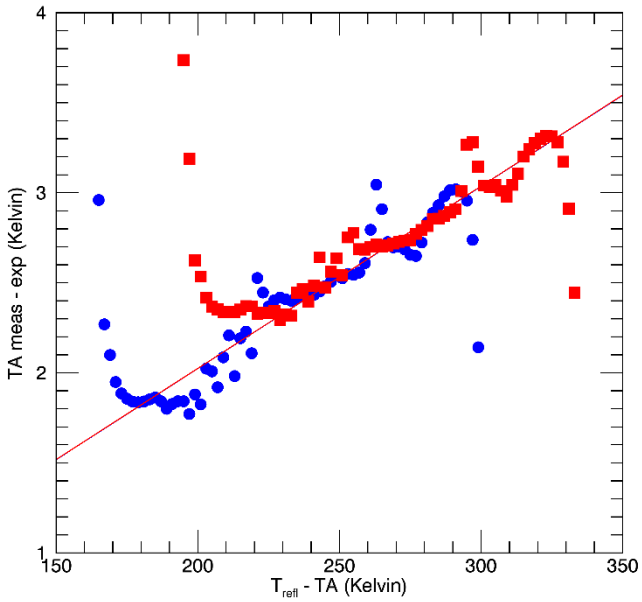

Figure 4: Regression of T_A measured minus expected versus binned $T_{refl} - T_A$. T_{refl} is the physical temperature of the antenna (from the JPL thermal model). TA is the radiometric antenna temperature. Blue: V-pol. Red: H-pol. The slope of the linear fits is the reflector emissivity. The bin population (not shown) is very small at the lower and upper end of the x-axis interval, which causes the outliers.

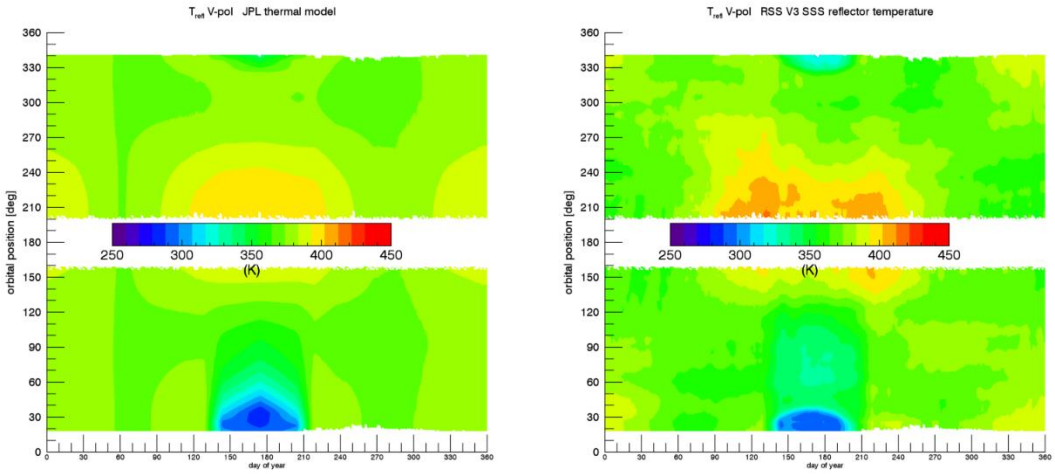

Figure 5: Physical temperature T_{refl} of the reflector. Left: JPL thermal model that is used in the SMAP L1B files (Piepmeier et al. 2023). Right: Reflector temperature in the RSS SMAP Version 3 release after the empirical adjustment ΔT_{refl} has been added.

The value of the reflector emissivity ε_{refl} can be determined by performing a linear regression of the SMAP $\Delta T_A = T_{A,meas} - T_{A,\exp}$ against $T_{refl} - T_A'$ before performing any correction for the emissive reflector. The slope of this regression is ε_{refl}. We have determined values of $\varepsilon_{refl} = 0.01012$, for both V-pol and H-pol (Figure 4). Similar values are used in the Version 4 L1B files (Piepmeier et al. 2023). It is worth noting that these values for the reflector emissivity are about 4 times larger than the values that were determined pre-launch.

There are no direct measurements of the physical temperature T_{refl} of the SMAP mesh antenna. Instead, only a thermal model for the SMAP reflector, which was developed and run by the Jet Propulsion Laboratory (JPL) thermal modeling team, is available (Figure 5 left). The values of this JPL thermal model are used and included in the SMAP L1B files (Piepmeier et al. 2023). Our analysis has revealed that the JPL thermal model is not accurate enough to retrieve ocean salinity from SMAP without adjustments. This can be seen from the Hovmoeller diagram in Figure 6, which shows the bias of $T_{A,meas} - T_{A,\exp}$ as function to time (day of the year) and orbital position (z-angle) using the JPL thermal model in the emissive reflector correction. In the computation of $T_{A,\exp}$ for V3 onwards we have used Scripps ARGO as reference salinity. The zonal and temporal biases increase significantly when the spacecraft goes in and out of solar eclipse during the summer months (these biases are also present during the winter months). In those instances, rapid cooling or heating of the SMAP reflector occurs. According to our analysis, the thermal models can both overestimate and underestimate the rate of these thermal changes. The observed zonal and temporal biases in Figure 6 are largely independent of the SMAP look direction. These biases differ significantly between ascending (lower half of the diagram) and descending (upper half of the diagram) swaths because the thermal heating and cooling of the SMAP antenna are not symmetric between the two swaths. This leads us to believe that these biases are indeed caused by inaccuracies in the JPL thermal model rather than by other sources such as galaxy correction or sun intrusion, which would strongly depend on look direction. It also seems unlikely that these biases are due to errors in dielectric model or surface roughness correction since these are expected to be largely the same in the ascending and descending swaths. The decision was made to apply an empirical adjustment to the JPL thermal model for the SMAP V3 salinity retrievals. The purpose of this adjustment is to minimize the zonal and temporal biases in $\Delta T_A = T_{A,meas} - T_{A,\exp}$ when the correction for the emissive reflector is performed with this empirical adjusted model. This was done by taking the values for the ΔT_A biases from Figure 6 and computing the corresponding value of ΔT_{refl} from equation (3). The empirical ΔT_{refl} depends on time (day of the year) and orbital angle (z-angle). The same empirical correction is used for all years. The result for the empirically adjusted thermal model in the SMAP V3 salinity release is shown in Figure 5 (right). We use the same thermal model adjustments for V-pol and H-pol. The values of ΔT_{refl} are included in the L2C files.

SMAP V4 and V5 use the same reflector emissivity and reflector temperature adjustment as V3.

In our approach to empirically determine both ε_{refl} and T_{refl} for SMAP, we have tried to avoid folding potential errors in one quantity into the other. When determining the value of ε_{refl} from the linear regression (Figure 4), we only used cases where the JPL thermal model was determined to be accurate i.e., where the biases in Figure 6 are small (less than 0.1 K).

In the releases prior to V3, the HYCOM SSS field was used to derive ΔT_{refl} . This resulted in significant temporal and zonal biases when compared to in-situ data. The main origin of these biases was the HYCOM field.

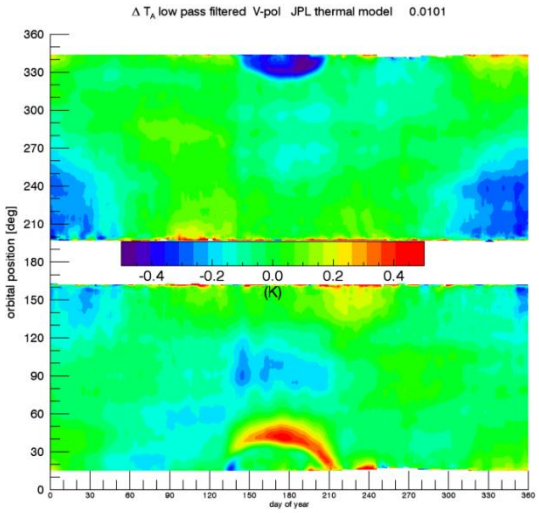

Figure 6: Hovmoeller diagram of SMAP TA measured - expected over the open ocean using the JPL thermal model for the SMAP mesh antenna. The x-axis is time (day of the year), and the y-axis is orbital position (z-angle). For the computation of TA expected we have used Scripps ARGO as reference salinity. The computation of this diagram is based on 2 years of SMAP data (September 2015 – August 2017). A simple spatial and temporal low-pass filter was applied by performing a running average in both dimensions.

4.3.2 Salty Biases at High Northern Latitudes and Correction for Emissive SMAP Antenna in V6

SMAP V5.0 shows salty biases compared to ARGO at high N latitudes (Figure 7). The biases have a seasonal variability.

In order to mitigate these biases, which do not depend on looking angle, a small adjustment to the physical temperature of the reflector antenna (Figure 8) is done in V6. The adjustment is slightly different for V-pol and H-pol.

The effect of this adjustment on the observed biases is shown in Figure 9. The salty biases at high N latitudes have largely disappeared.

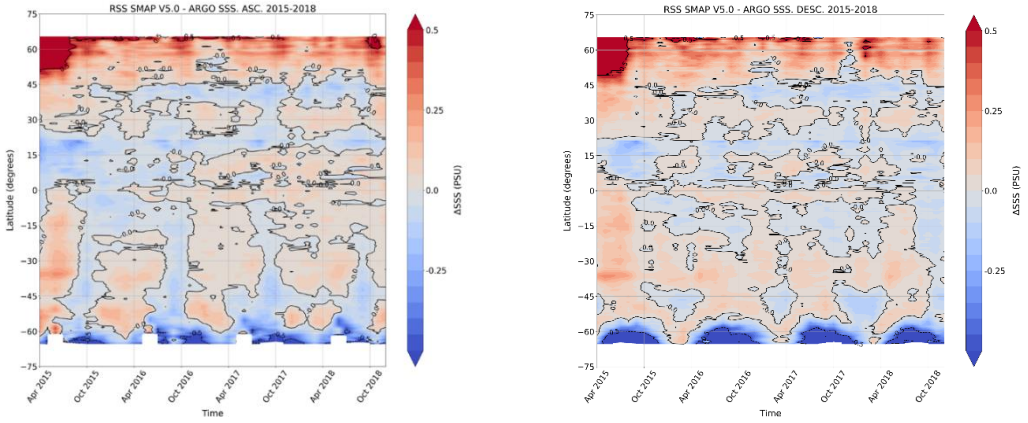

Figure 7. Hovmoeller plot of SMAP V5.0 – ARGO SSS. Left: ascending swath. Right: descending swath.

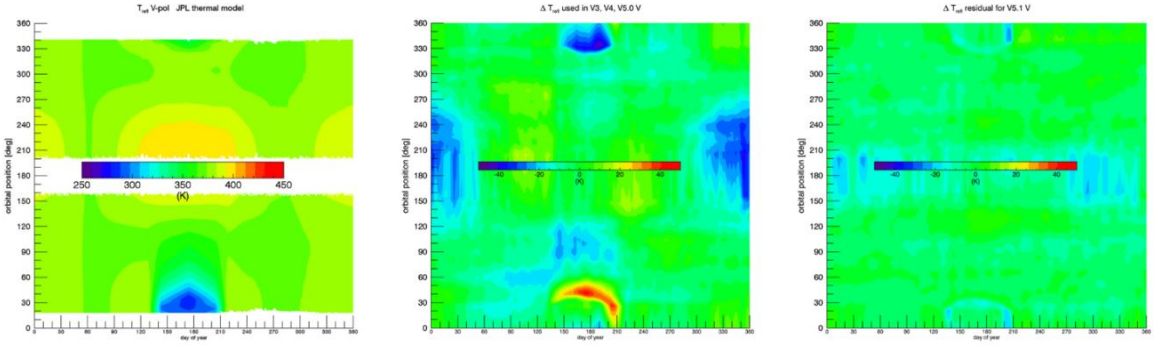

Figure 8. Physical temperature of the reflector antenna (in Kelvin). Left: According to the JPL thermal model. Center: Adjustments that were done for the V3 – V5 SSS releases. Right: Additional adjustment for the V6 release shown for the V-pol.

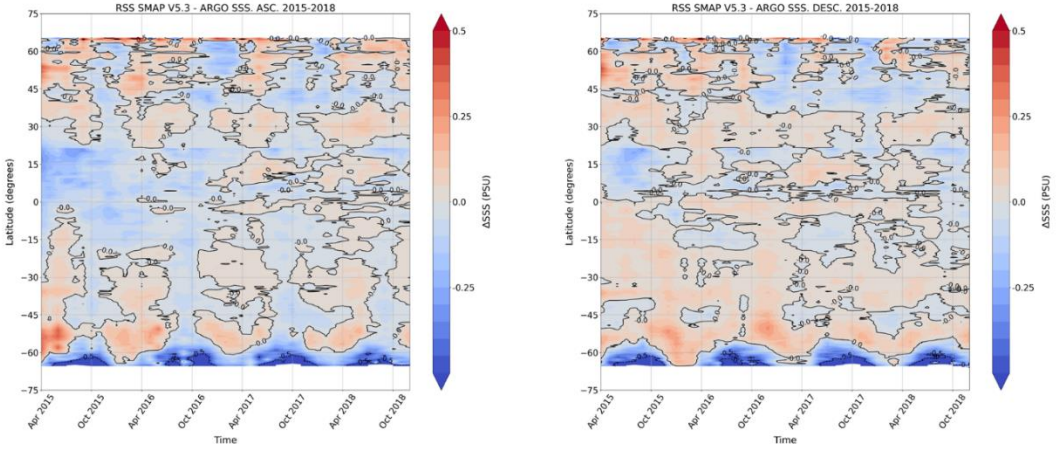

Figure 9. Hovmoeller plot of SMAP – ARGO SSS after adjusting the physical reflector temperature. Left: ascending swath. Right: descending swath.

4.4 Atmospheric Oxygen Absorption

The SMAP V2 release used the oxygen absorption model by Wentz and Meissner (2016). The SMAP V3 release uses the oxygen absorption model by Liebe et al. (1992), as does the Aquarius Version 5 release. SMAP V4, V5, and V6 use the same oxygen absorption model as V3.

4.5 Correction for Reflected Galaxy

4.5.1 Correction for Reflected Galaxy in V3 – V5

The correction for the reflected galaxy uses a combination of the geometric optics model for reflection from rough ocean surfaces and the results from the SMAP for – aft look analysis. It is described in detail in Meissner et al. 2017 and Meissner et al. 2018. The empirical zonal symmetrization that was done in the Aquarius Version 5 release was **not** done for the SMAP V3 release. The SMAP V4 and V5 releases use the same reflected galaxy correction as V3.

4.5.2 Look Angle Dependent Biases and Correction for Reflected Galaxy in V6

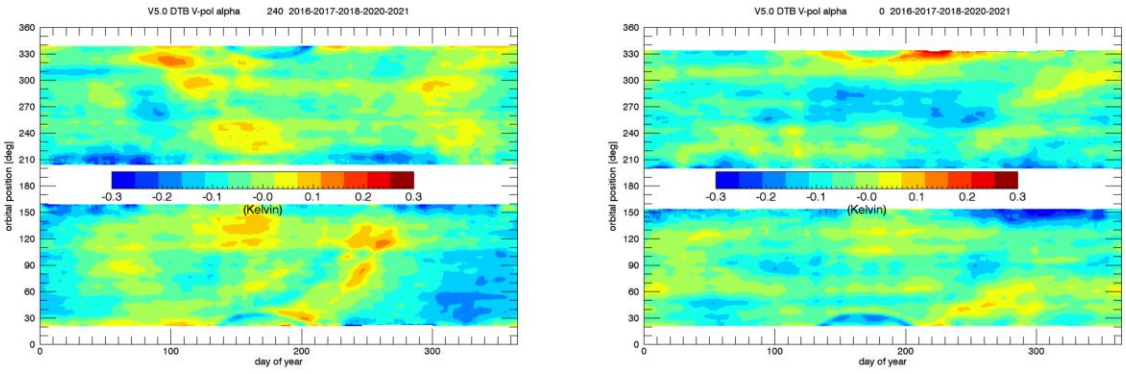

Figure 10. Hovmoeller plots for TB measured – expected V-pol during 2017. Left: Looking right of forward (look angle 240^{o}). Right: Looking forward (look angle 0).

Up to and including V5.0, the SMAP L2C salinity data exhibit biases that depend on the look direction relative to forward. The biases change with time of year but show little intra-annual variability (see Figure 10). The effect is most prevalent at high Southern latitudes, but it is observed globally.

A detailed analysis shows that these biases are largely caused by residual reflected galactic radiation in the current SMAP salinity retrieval algorithm.

This issue is demonstrated in Figure 11. The red circled area shows an instance where the reflected galaxy TA is very small (0.1 – 0.2 K). However, it does not vanish completely. This small residual galaxy led to a bias in TA measured – expected. This is the cause of the fresh salinity bias that is observed in the Hovmoeller diagram for the right of forward look (left panel in Figure 10).

The largest part of the observed directionally dependent salinity biases can be tracked down to small biases in the reflected galaxy TA.

It was also found that the observed directional biases only weakly depend on surface wind speed. This suggests using the observed TA measured – expected in the right ascension galactic system (right panel in Figure 11) as the basis for a small adjustment to the galaxy correction that will be applied in the SMAP V6 salinity retrieval algorithm.

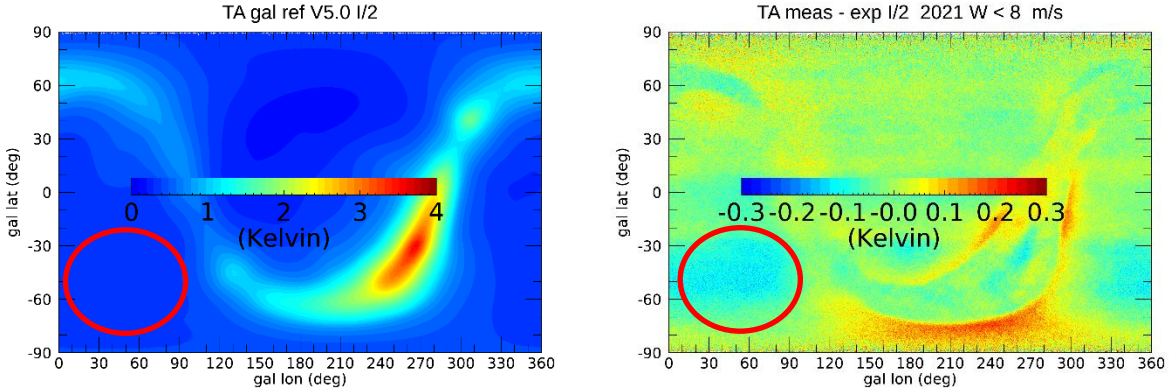

Figure 11. Left: Total reflected galactic radiation. Right: TA measured – expected (for the year 2021). The plots are done in the Earth centered right ascension system for Y2000: X-axis pointing into the direction of the vernal equinox, Z-axis = Earth-axis. The galactic longitude (gal lon) is the azimuth angle in this coordinate system. The galactic latitude (gal lat) is the polar angle in this coordinate system and coincides with the standard geodetic latitude.

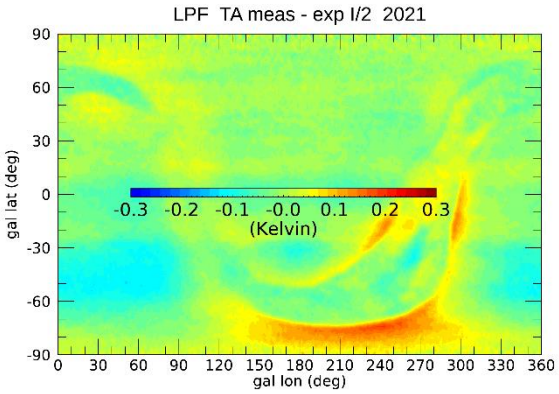

Figure 12. Adjustment to the reflected galactic correction that is applied in the salinity retrieval algorithm. It is obtained by low-pass filtering the TA measured – expected (right panel in Figure 11).

For the V6 release, an adjusted correction for the reflected galaxy was derived by low-pass filtering the observed TA measured – expected in the galactic right ascension system (right panel in Figure 11). The result is shown in Figure 12, and it is added as an additional correction in the V6 salinity retrieval algorithm.

Figure 13 shows the result after this adjusted correction is applied. The observed TA biases in the right of forward look are indeed mitigated significantly when compared to Figure 10.

Figure 14 shows the improvement of the SMAP – ARGO salinity for the right of forward look in November 2016 when this adjustment to the reflected galaxy is applied.

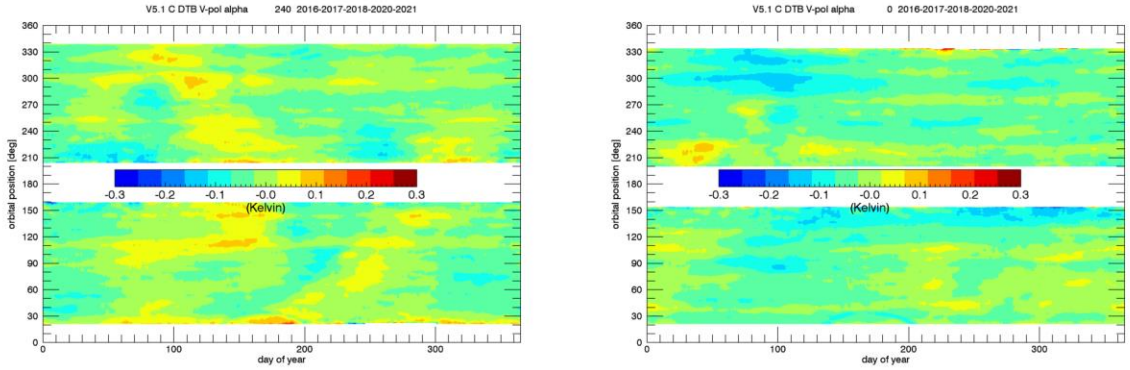

Figure 13. As in Figure 10 after applying the adjustment to the reflected galaxy from Figure 12.

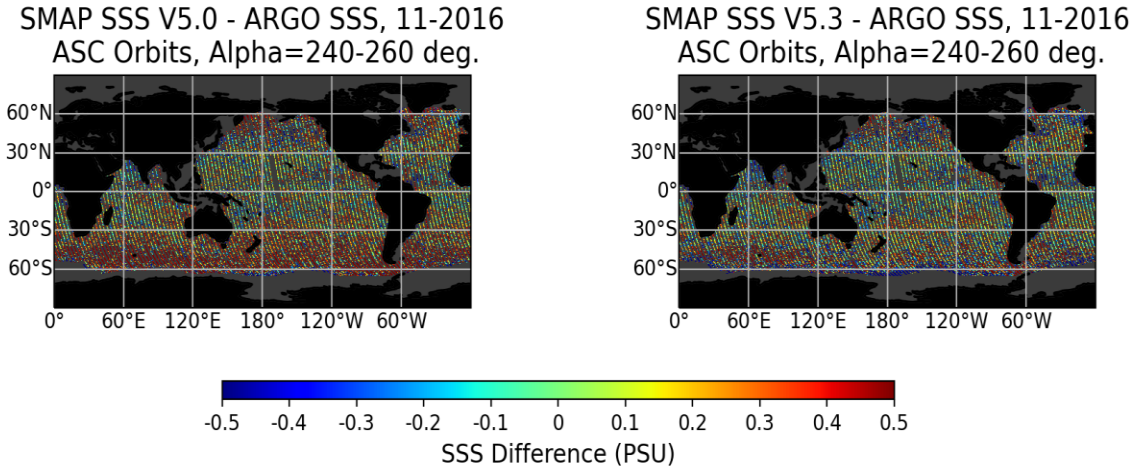

Figure 14. SSS SMAP – ARGO during November 2016 when looking right or forward. Left: V5.0. Right: After the adjusted reflected galaxy correction has been applied (V6.0).

4.6 Antenna Pattern Correction (APC)

The matrix $\mathbf{A}$ (whose elements for the V5 and V6 salinity releases are shown in Table 3) transforms the Stokes vector of the Earth TA into TOI (top of the ionosphere) TB (Meissner et al. 2017):

$$\mathbf{T}_{\mathbf{B,TOA}} = \mathbf{A} \cdot \mathbf{T}_{\mathbf{A,Earth}} \quad (4)$$

The SMAP 4x 4 A-matrix elements are computed from SMAP pre-launch antenna patterns that have been created by the JPL antenna group from the GRASP software (file *SMAP_Antenna_Pattern_verF_Freq1413_Ang000_2D.dat*, provided by Emmanuel Dinnat, GSFC).

Table 3: A-matrix elements A_{ij} (in I, Q, S3, S4 basis) of the SMAP V5 and V6 releases. The entries in red denote matrix elements that differ from the pre-launch computation.

	j=1	j=2	j=3	j=4
i=1	1.1046	-0.0001	0.0036	-0.0006
i=2	0.0000	1.1349	+0.0066	-0.0001
i=3	0.0009	0.0042	1.1336	-0.0553
i=4	0.0003	0.0014	+0.0117	1.1297

For the SMAP salinity retrievals, we have adjusted some of the A-matrix elements. These adjustments were done in order to:

1. Get the best TB over ocean scenes and the Amazon rainforest for all 4 Stokes parameters (I, Q, S3, S4).
2. Minimize spurious observed cross-talk dependencies between I, Q and S3, S4.

The non-linear IU coupling that was observed in the Aquarius data (Meissner et al. 2017) is not observed with SMAP.

4.7 Ocean Target Calibration

The ocean target calibration (Meissner et al. 2017, 2018) removes any remaining, constant, and time-varying biases in the TA measured – expected over the open ocean. We calculate the 3-day running average of TA measured – expected $\langle \Delta T_A(i) \rangle = \langle T_{A,meas}(i) - T_{A,\exp}(i) \rangle$ as well as the average $\langle T_A(i) \rangle$ for each orbit i over the open ocean for rain free scenes. The computation of TA expected uses HYCOM as reference salinity.

For the V5 and V6 releases we do not include observations for which:

- The gain weighted land fraction g_{land} exceeds 0.0005 or the land fraction within the 3-dB footprint f_{land} exceeds 0.001 (land contamination).
- The observation is not within sea-ice zone 0 (section 5.3, sea-ice contamination).
- The IMERG rain rate exceeds 0.1 mm/h (rain contamination).
- The sun glint angle is below 50° and the scan angle is between 30° and 150° (conservative sun glint flag, see section 5.2).

- The moon glint angle is below 15°
- The TA of the reflected galaxy (average of V and H-pol) exceeds 1.0 K.

The values of $\langle \Delta T_A(i) \rangle$ and $\langle T_A(i) \rangle$ are included in the metadata of the L2 files. We assume that any remaining calibration adjustment is an effective adjustment of the noise-diode temperature T_{ND}. If T_{Ap} is the antenna temperature of a SMAP observation for polarization p = V or H after correcting for the emissive reflector, then we calculate the *calibrated antenna temperature* $T_{Ap,cal}$ as:

$$T_{Ap,cal} = T_{Ap} - \frac{\langle \Delta T_{A,p}(i) \rangle}{\langle T_{Ap}(i) \rangle - \langle T_D \rangle} \cdot \left(T_{Ap} - \langle T_D \rangle \right) \qquad p = V, H \tag{5}$$

The $\langle T_D \rangle$ in equation (5) stands for an average value of the Dicke load temperature. For our purposes, we set this to a value of 293 K. Per construction, the running 3-day average of $\Delta T_{Ap,cal}$ is zero for each orbit: $\langle \Delta T_{Ap,cal}(i) \rangle = 0$.

We have also found small offsets for the S3 and S4, which are constant in time after the SMAP radar was shut off but differ during the time period before that. The following offset correction for S3 and S4 is performed:

$$T_{Ap,cal} = T_{Ap} - \langle T_{Ap,offset} \rangle \quad p = S3, S4 \tag{6}$$

The offset values $\langle T_{Ap,offset} \rangle$ are +0.22 K (for S3) and -0.43 K (for S4).

4.8 Correction of Early Mission Biases in V6

In V5 and earlier versions, strong salty biases in the SMAP SSS retrievals are observed at many locations near the continental shelves during April 2015 – August 2015 (Figure 15 - Figure 16).

These biases are related to the operation of the SMAP radar during this period. Specifically, they can be traced back to the data acquisition mode. Since August 2015 (shortly after the SMAP radar shutoff)), the SMAP radiometer has been operating in high-rate (HR) data collection mode, which utilizes the sub-band division of the SMAP L-band. While the radar was turned on and operational (April 2015 – August 2015), the HR acquisition was only applied for land scenes that were used in soil moisture retrievals. In order to save bandwidth during the data downlink, the radiometer operated in low-rate (LR) mode over most of the open ocean. The LR acquisition used only the full band of the SMAP L-band channel. Shortly after the failure of the SMAP radar only HR acquisition has been used consistently for all scenes.

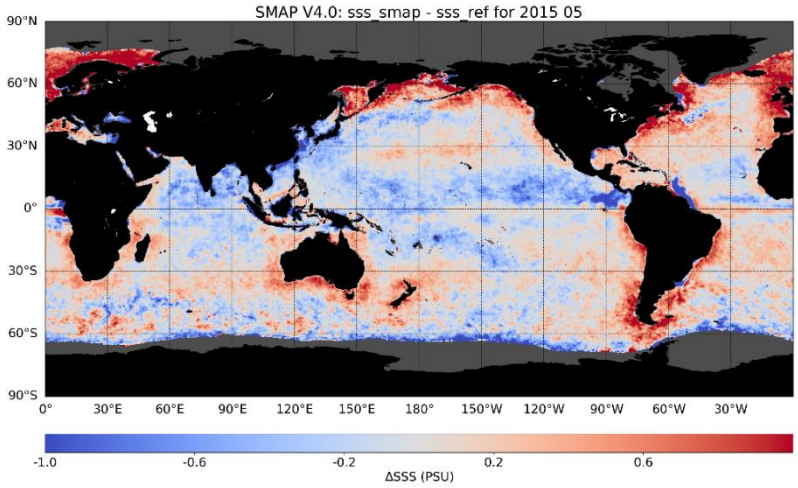

Figure 15. SMAP – HYCOM salinity during 05 2015. Large salty biases around large parts of the continental shelves are evident.

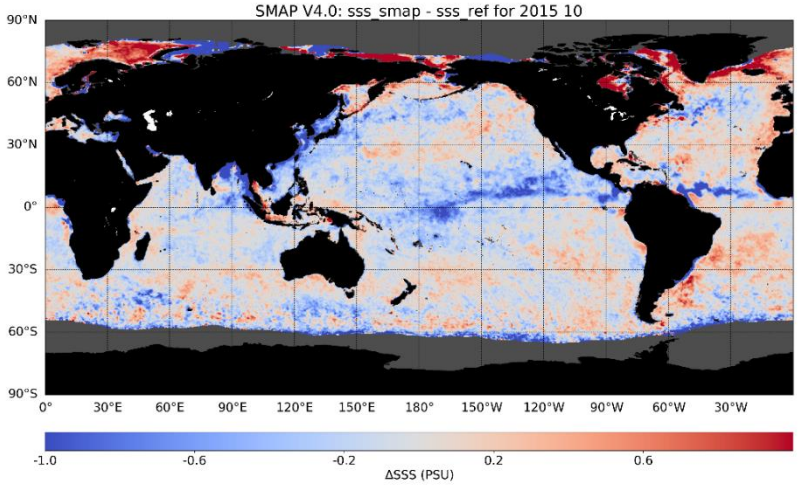

Figure 16. SMAP – HYCOM salinity during 10 2015. The salty biases around the continental shelves have disappeared.

The L1B SMAP data contain a flag that indicates if the radiometer is operating in HR or LR mode (Figure 17). In the early parts of the mission, the switch between the two modes would occur as the satellite passed over the continental shelves. This means that, close to the continental shelves, the instrument was already (or still was) in HR mode even if it was observing the open ocean.

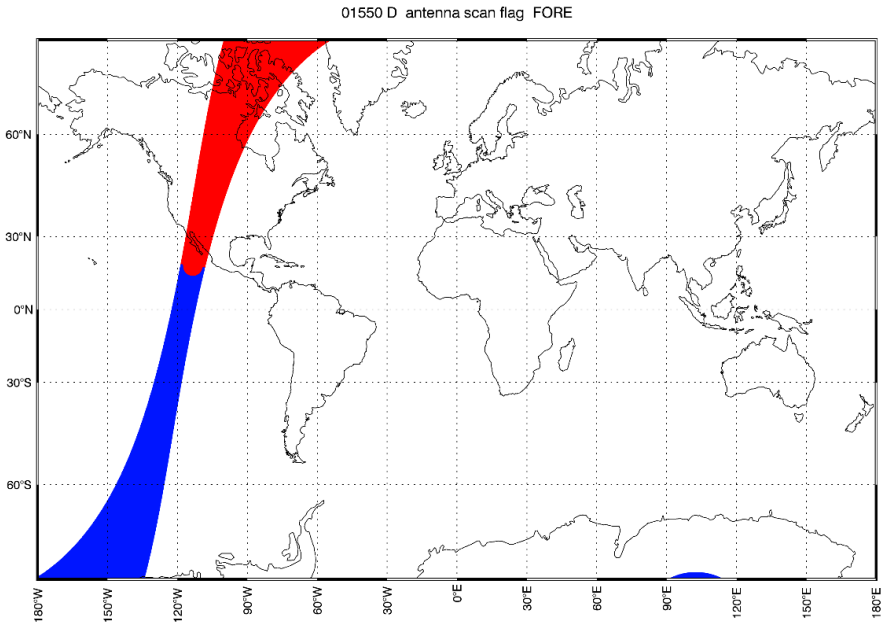

Figure 17. Flag indicating high-rate (HR, red) and low-rate (LR, blue) radiometer data acquisition.

An analysis of measured – expected antenna temperatures (TA) separately for LR and HR modes (Figure 18 + Figure 19) was performed. This analysis revealed that there is an apparent offset (bias) in the TA between the 2 modes. The HR TA are about -0.25 Kelvin lower than the LR TA. This is the case for all 4 Stokes parameters: V-pol, H-pol, 3rd Stokes, and 4th Stokes. The result of these TA biases are salty biases in the SMAP SSS retrievals during HR acquisition compared to LR acquisition. These biases manifest themselves as salty "halos" around the continental shelves where the satellite would switch data collection modes. We note that part of the SSS retrieval algorithm is to perform a dynamic ocean target calibration of the TA, which globally debiases the TA over the open ocean.

The mitigation of these salty biases in Version 6 consists of:

1. Saving the quality flag in the low-level data, which indicates the HR/LR acquisition mode, for the salinity retrieval algorithm.

2. De-biasing the HR TA relative to the low-level TA before any resampling is done. The numerical values of the shifts that are applied are -0.26 K (V-pol), -0.24 K (H-pol), -0.25 K (S3), -0.26 K (S4).

3. Performing the dynamic ocean target calibration on the de-biased fields.

The result is shown in Figure 20.

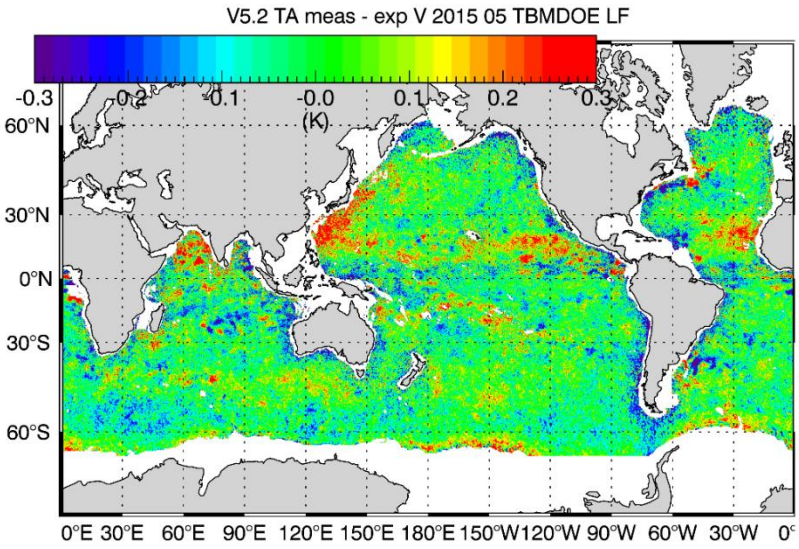

Figure 18. Measured – expected TA for LR mode during 05 2015.

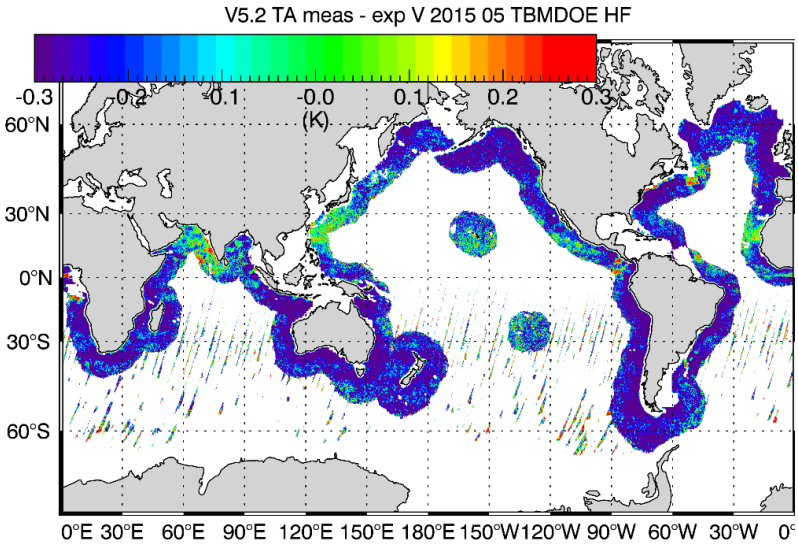

Figure 19. Measured – expected TA for HR mode during 05 2015.

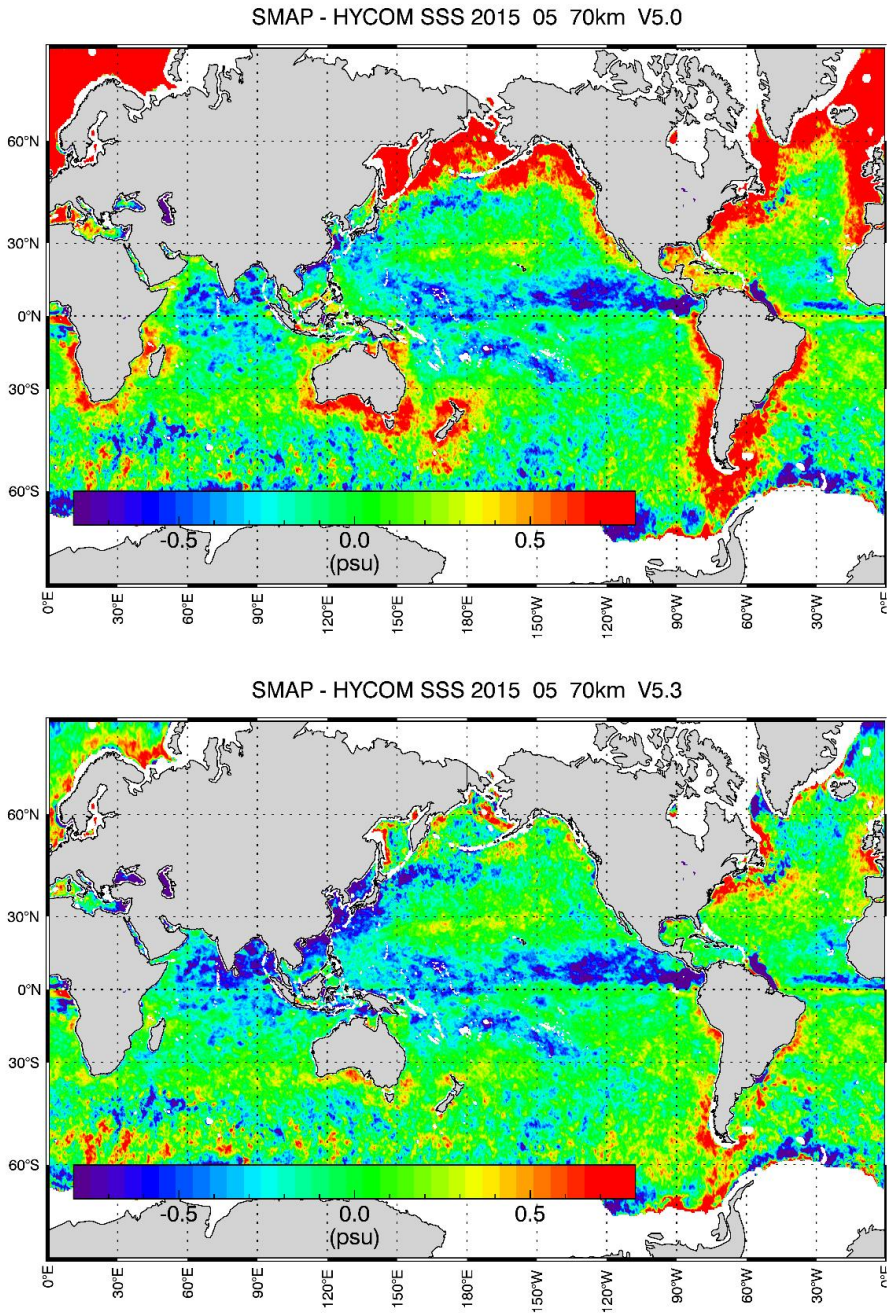

Figure 20. SSS SMAP 70-km – HYCOM for May 2015. Upper: V5.0. Lower: after de-biasing the LR versus HR TA (V6.0).

5 SMAP SALINITY RETRIEVALS IN DEGRADING CONDITIONS

5.1 Sidelobe Correction to Mitigate Land Intrusion

The V5 and V6 releases use the same sidelobe correction for land intrusion as V4. This correction is described in the following section.

5.1.1 Computation of the SMAP Sidelobe Correction

The Aquarius and SMAP salinity retrievals degrade quickly as the footprint gets within 500 km of land. This land-contamination error occurs because the land is radiometrically much warmer than the ocean. When the satellite observation gets close to land, a correction for land entering **the antenna sidelobes can be derived from simulated Aquarius and SMAP brightness temperatures** (Meissner et al. 2017, 2018).

The land contamination is most conveniently dealt with at the TOA (top of the atmosphere). The error due to this contamination is given as:

$$\Delta T_{B,TOA} = \hat{T}_{B,TOA} - \overline{T}_{B,TOA,ml} \tag{7}$$

The 1st term on the right-hand side of equation (7) is the simulated value of the actual *observed* (i.e., measured) signal. It is computed by simulating TOA Earth brightness temperatures containing representative ocean and land scenes and integrating them over the full SMAP antenna gain pattern. In the simulation, we use the pre-launch SMAP antenna pattern that was provided by the SMAP antenna group at JPL. The 2nd term of the right-hand side of equation (7) is the *true* TOA TB coming from the antenna main beam. Using the simulated SMAP TB, a table of the $\Delta T_{B.TOA}$ is computed one time off-line before the algorithm is run. In addition, the antenna gain weighted land fraction g_{land} is computed by integrating the antenna gain over the land covered area.

When computing the values for g_{land} and $\Delta T_{B,TOA}$ in the SMAP Version 2 release, it was assumed that the position of the equatorial crossing repeats itself exactly every 8 days. This assumption is not accurate because there are small shifts in the equatorial crossing position from the target position. This has resulted in inaccuracies in the salinity retrievals near the coast after the land correction is applied.

Beginning with Version 3, the computation of g_{land} and $\Delta T_{B,TOA}$ no longer operates under this assumption. Rather, we are keeping the equatorial crossing as a degree of freedom as was done in the Aquarius Version 5 land correction (Meissner et al. 2017; 2018). Because SMAP performs a full 360° scan, the sidelobe correction needs to be derived for a series of different scan positions.

5.1.2 Major Changes in the Version 4 Sidelobe Correction

The spatial (latitude/longitude) resolution of the land tables was increased to 0.125 º in Version 4.0 from 0.5 º in Version 3.0 (validated release) and 0.25 º in Version 3.3 (evaluation version). See Figure 21 for the effect of the spatial resolution of the land tables on the performance of the salinity retrieval algorithm near land.

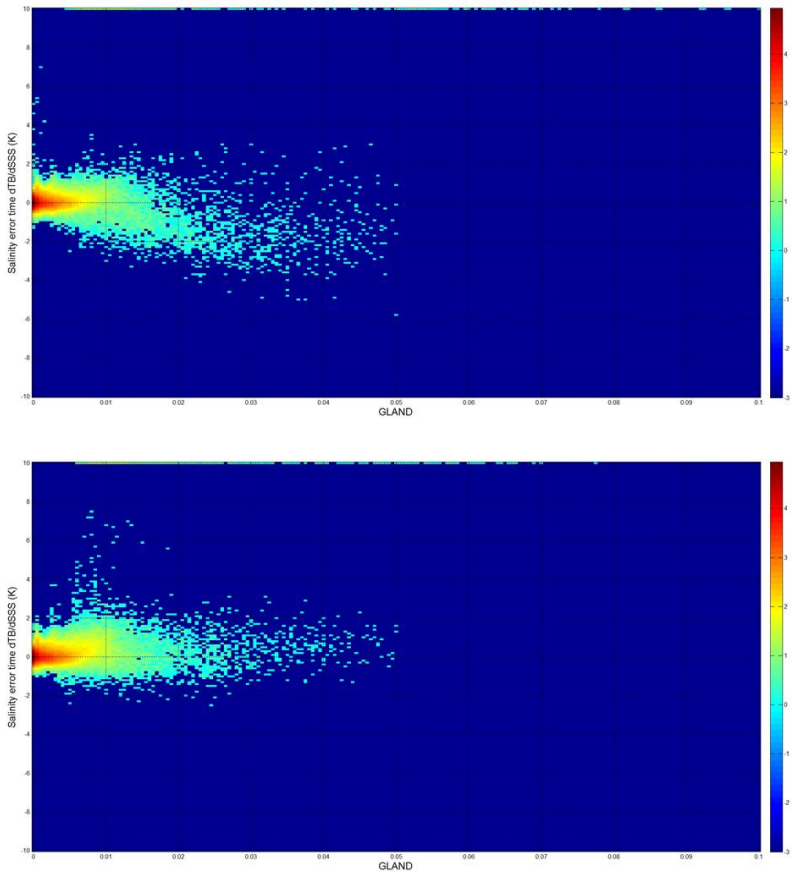

Figure 21: SMAP – HYCOM salinity SSS, converted to ΔTB by multiplying with the sensitivity $\frac{dTB}{dSSS}$, as a function of *gland* (antenna gain weighted land fraction). The x-axes are gland between 0 and 0.1 in increments of 0.01. The y-axes are ΔTB from -10 K to + 10 K in increments of 2 K. The value of sensitivity depends on SST and SSS. Its computation is based on the dielectric model (Meissner and Wentz 2004, 2012). Upper: Using a 0.25º land correction table as in Version 3.3. There is overcorrection resulting in negative ΔTB. Lower: Using a 0.125 º land correction table as in Version 4.0. Note that the scatter at higher values of *gland* is also reduced with the Version 4.0 0.125 º land correction. Also, note that the values of gland (x-axes) themselves change when increasing the resolution of the land correction tables.

The g_{land} and $T_{B,TOA}$ land correction tables in SMAP Version 4.0 depend on:

1. Polarization (v-pol, h-pol).
2. Cell longitude (2880 elements in 0.125º increments).
3. Cell latitude (1441 elements in 0.125º increments).

4. Ascending/descending (2 elements).
5. Scan angle (30 elements in 12° increments).
6. The $T_{B,TOA}$ land correction tables also depend on time (12 months). The g_{land} tables do not.

These variables result in the SMAP V4.0 $T_{B,TOA}$ land correction table having a dimensionality of (2, 2880,1441, 2, 30, 12).

The computation of the g_{land} and $T_{B,TOA}$ land correction tables in SMAP Version 4.0 based on the orbit simulator follows the same basic procedure as in Aquarius Version 5 (Meissner et al. 2017, 2018).

Starting with V5.0, the land correction is not applied if the values of either gland or fland exceed 0.1, which is defined as strong land contamination (bit 2 of Q/C flag set, section 6).

5.1.3 Land Surface Emissivity

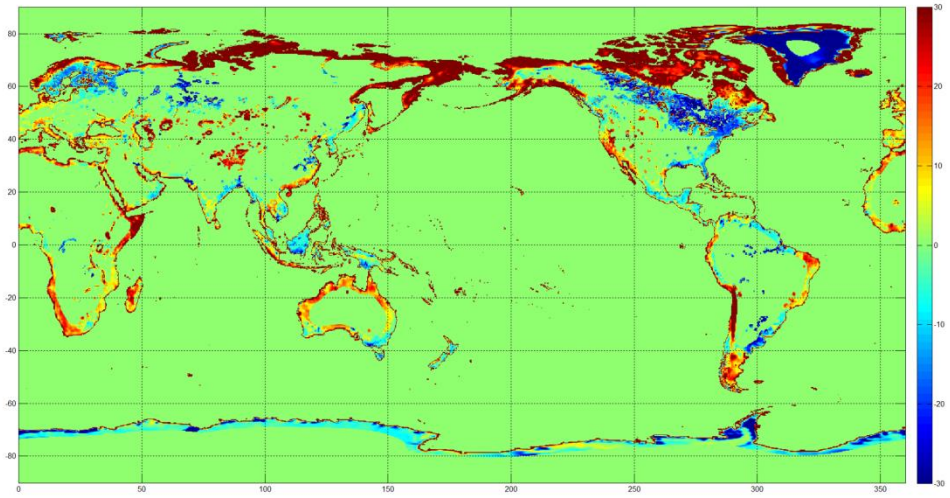

Figure 22: SMAP measured land TB minus land-emission model TB (based on NCEP soil moisture and land surface temperature).

For calculating the sidelobe correction near land it is necessary to know the TB that is emitted from the land surface. Up to and including Versions 3.0/3.3, we used a land surface emission model based on soil moisture and land surface temperature values from NCEP. In many coastal areas, the NCEP data for soil moisture are poor or non-existent. This resulted in significant errors in certain areas e.g., the Aleutian Islands, the Gulf of Maine, and Baja California. The land emission in V4.0 is based on a 12-month climatology of SMAP TB over land.

SMAP measures TA over land in the coastal areas, which is contaminated by emission from the ocean through sidelobes. This contamination needs to be removed in order to obtain SMAP land surface TB. This can be used in the derivation of the land tables. The basic procedure is the same as removing the land contamination from an ocean observation near the coast. If the

gain-weighted ocean fraction in the cell over land is g_{ocean} = 1 - g_{land}, then the measured (ocean contaminated) TB is approximately given by:

$$T_{B,meas} = (1 - g_{ocean}) \cdot T_{B,land} + g_{ocean} \cdot T_{B,ocean} \quad (8)$$

The value of g_{ocean} = 1 - g_{land} can be computed from the ocean simulator (section 5.1.1). The ocean TB has a much smaller dynamic range than the TB over land. We can therefore assume typical values for the $T_{B,ocean}$ (121 K for V-pol, 86 K for h-pol) in (8) and then solve (8) for $T_{B,land}$ in order to remove the ocean intrusion into the land scenes.

The difference between SMAP land TB and the NCEP based land model TB can reach 20 K in some areas (Figure 22).

5.1.4 Additional Empirical Corrections

Two additional empirical corrections were added in the sidelobe correction of the Version 4.0 release. They were derived so that globally the TB measured minus expected curves become flat as function of g_{land}.

1. A term that is proportional to δ_2 , which is the deviation of the *spatial gradient of gland* from a strictly linear gradient.

$$\Delta T_{B1} = \begin{pmatrix} \Delta T_{B1,V-pol} \\ \Delta T_{B1,H-pol} \end{pmatrix} = \begin{pmatrix} 150 \cdot \delta_2 \\ 160 \cdot \delta_2 \end{pmatrix} \quad (9)$$

The value of $\delta_2(i, j)$ at a grid point (i, j) of the 1/8° grid of the land correction tables is determined as:

$$\delta_2 = \left[\frac{1}{9} \cdot \sum_{\substack{k=i-1,i+1,1 \\ l=j-1,j+1,1}} g_{land}(k,l) \right] - g_{land}(i,j) \quad (10)$$

If g_{land} at the cell (i, j) is a strict linear function in 2-dimensional space, then $\delta_2 = 0$. For the simple case of only 1 spatial dimension as degree of freedom, the value of δ_2 is characteristic for the 2nd derivative of g_{land} as function of spatial distance from the coast. When getting very close to the coast, the value of g_{land} increases very rapidly as function of distance from the coast. This generally results in an over-correction error when doing a linear interpolation between the grid cells of the land correction tables. The size of this error depends on the spatial resolution of the land correction tables. In V3, where the spatial resolution of the land table was only ½°, this caused a large error close to the coast, which made the land correction basically useless. Even in V4, where the spatial resolution of the land correction is 1/8° a residual error remains. The purpose of the correction (9) is to compensate for this error.

2. An empirical term that increases linearly with *gland* above 0.02.

$$\Delta T_{B2} = \begin{pmatrix} \Delta T_{B2,V-pol} \\ \Delta T_{B2,H-pol} \end{pmatrix} = \begin{pmatrix} 78 \cdot (g_{land} - 0.02) \\ 83 \cdot (g_{land} - 0.02) \end{pmatrix}, \quad g_{land} > 0.02 \tag{11}$$

If $g_{land} < 0.02$ the ΔT_{B2} is set to 0. At $g_{land} = 0.04$, which is the largest value for land contamination that is regarded to give a useful salinity retrieval, the size of ΔT_{B2} is about 25% of the size of the sidelobe correction.

5.1.5 Land Exclusion for Calculating Smoothed Product

If the SMAP 3-dB footprint actually touches land, the sidelobe correction breaks down. In V4.0 we introduced an additional land contamination fraction, called *fland*, which is the percentage of land within the 3-dB footprint. This parameter is used for screening and flagging in addition to the gain weighted fraction *gland*. This becomes particularly important close to the many small islands in the Central Pacific.

The smoothed product *sss_smap* is obtained from the 40-km product *sss_smap_40km* by computing the next-neighbor average at each 0.25° grid cell. See section 2.10 equation (1). The next-neighbor average normally consists of the center cell plus 8 adjacent cells, but cells are excluded in the case of land contamination. Cells are excluded for land contamination if one of the following conditions apply:

1. The value of *gland* > 0.04.

2. The value of *fland* > 0.005. This value was increased in Version 5.0 compared to Version 4.0, where it had been set to 0.001.

If either of these conditions is true for a given cell, then it is not used in the next-neighbor average. The values of *gland* and *fland* are based on averages over all possible look angles in each Earth grid cell.

These conditions are defined as **moderate land contamination** (section 6).

Figure 23 shows monthly maps (05/2018) of SMAP – HYCOM SSS near the Baja of California for the V3.0, V3.3, and V4.0 70-km/smoothed products. In V3.0, areas within more than 100-km from the coast were flagged to avoid land contamination. Nevertheless, light land contamination is still visible near some coastal areas. In V3.3, the threshold for land contamination was increased, which resulted in strongly contaminated cells near the coast. In V4.0, we can retrieve SSS within 30 – 40 km from land. Other examples of the improvement in the land correction in V4.0 are shown in Figure 24, Figure 25 and Figure 26.

5.1.6 Results and Performance of Land Correction in Version 4.0

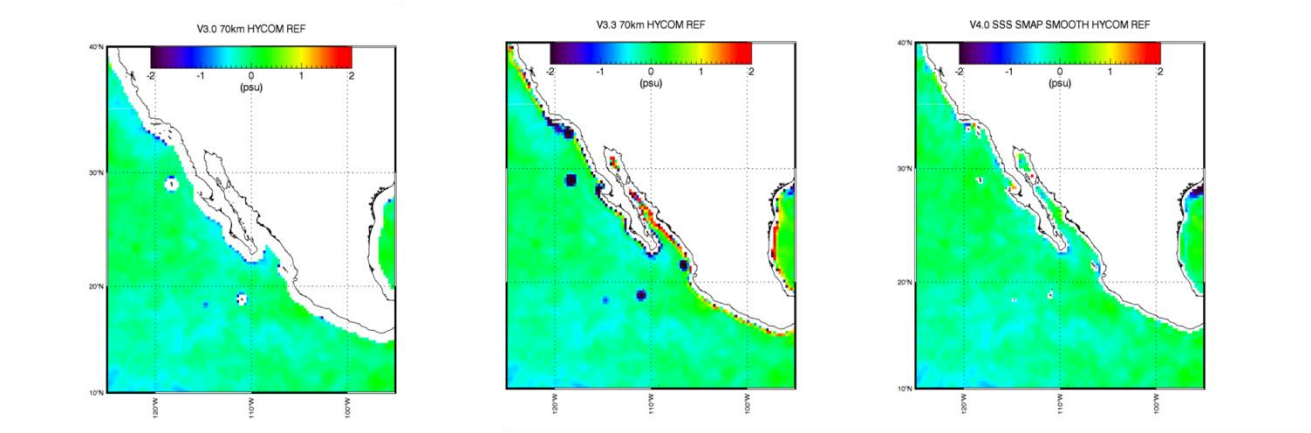

Figure 23: SMAP – HYCOM salinity near Baja California (May 2018). Left: Version 3.0 70-km product. A large area near the coast was flagged for land contamination. Center: V3.3 70-km product. Right Version 4.0 smoothed product.

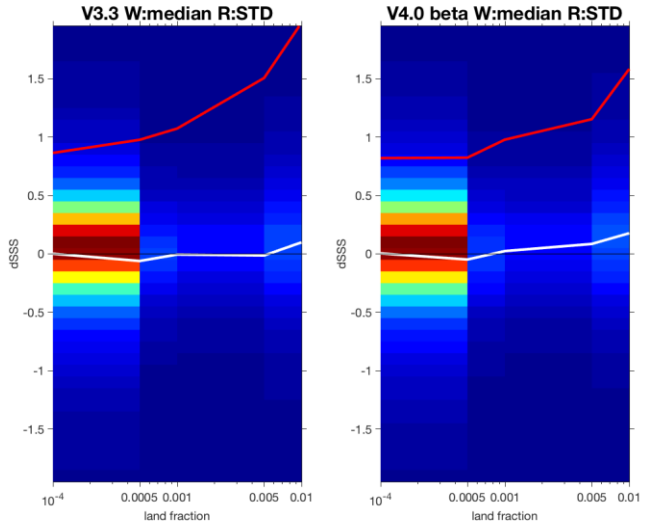

Figure 24: Statistics of RSS SMAP L2C versus ARGO match-ups as a function of gland. Left: V3.3. Right: V4.0. Median (white curve) and standard deviation (red curve). The colored shades indicate the 2-dimensional probability density. The analysis and figure were provided by H.-Y. Kao, ESR.

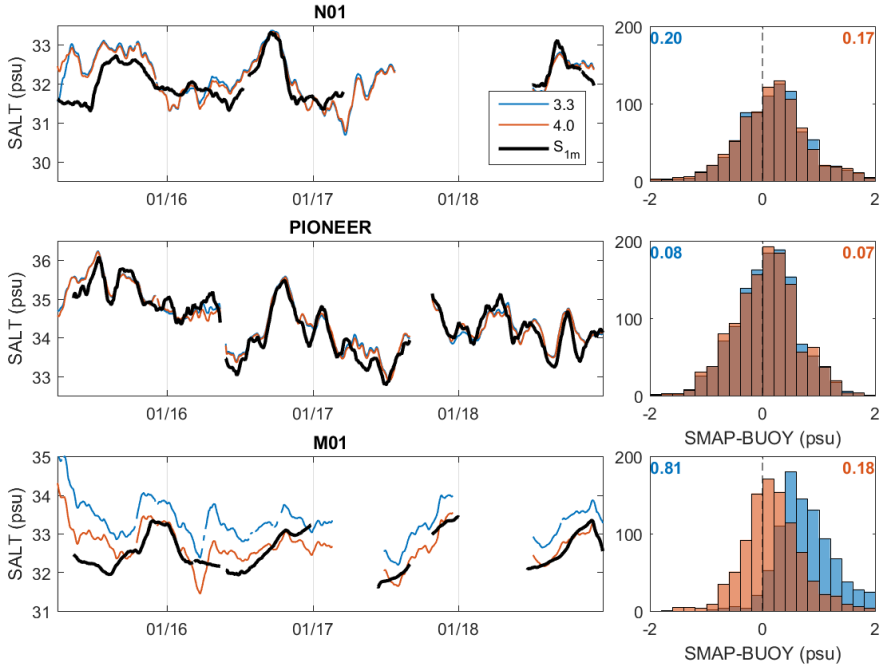

Figure 25: Improvement of land correction in V4.0 in Gulf of Maine area. The plots show comparison between SMAP and 3 moored buoys. The salty bias in SMAP V3 (blue) compared to Buoy M01 (black), which is close to the coast, is strongly reduced in V4 (red). The analysis and figure were provided by S. Grodsky, University of Maryland.

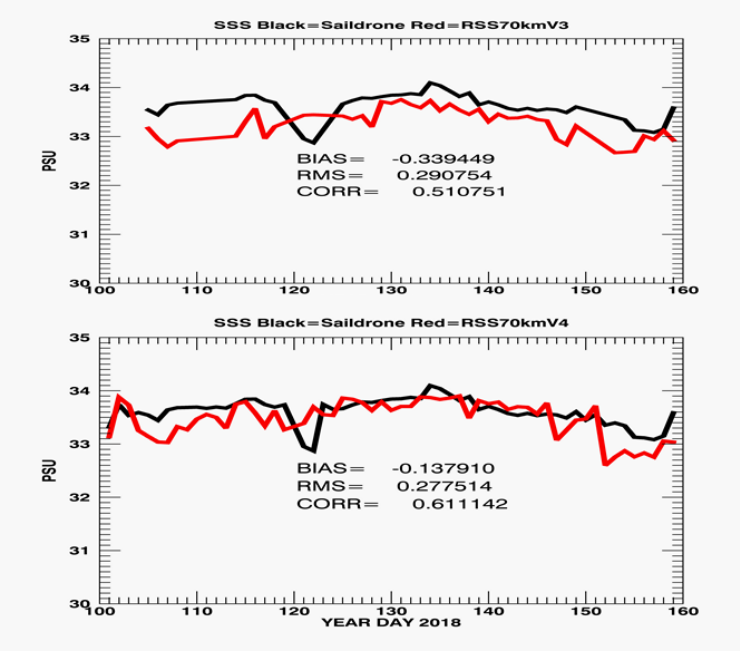

Figure 26: Comparison of SMAP SSS (8-day L3) and saildrone CTD salinity measurements during the Baja deployment (April 11 – June 11, 2018). For details see Vazquez-Cuervo et al. 2019. Upper: V3. Lower: V4. Black: saildrone. Red: SMAP. The fresh bias observed in V3 is greatly reduced in V4, in particular near Guadalupe Island. The analysis and figure were provided by J. Vazquez, JPL.

5.2 Sun-Glint

5.2.1 Sun Glint Flagging in V3 – V5

Due to the observation geometry of SMAP, at certain positions, there is only a small angle at the Earth surface between the direction of the SMAP antenna and the Sun. In these conditions, a portion of the Sun's brightness temperature is reflected off the ocean surface and into the SMAP field of view. The roughness of the ocean surface creates non-specular reflections so that solar contamination may be present at even modest sun glint angles.

A quality control (QC) flag is set in the SMAP L2C files when SMAP measurements may be affected by solar contamination. We found that the QC flag in SMAP V3 (and in prior versions) was too conservative: not only were bad measurements flagged, but measurements unaffected by solar contamination were also flagged, reducing the ocean coverage. For Version 4.0, we developed a revised QC flag that reduced false positives while still rejecting the contaminated measurements. This revised QC flag was also used in Version 5.0.

The sun glint QC flag in V3.0 was set when the sun glint angle is below 50° and when the scan angle is between 30° and 150°. The impact of the V3.0 sun glint QC flag is illustrated in Figure 27 and Figure 28, which display the mean of the residual SSS (defined as the difference between the retrieved salinity and the reference salinity) as a function of sun glint angle and wind speed. The figures show the data, respectively, without and with the sun glint QC flag used to mask out data.

While effective at removing the contaminated measurements, many un-contaminated measurements are also removed by the flag, especially at low winds. Furthermore, a discontinuity is present at the sun glint angle = 50° line, since a few measurements are present below that angle yet are outside the scan angle range of 30° to 150°.

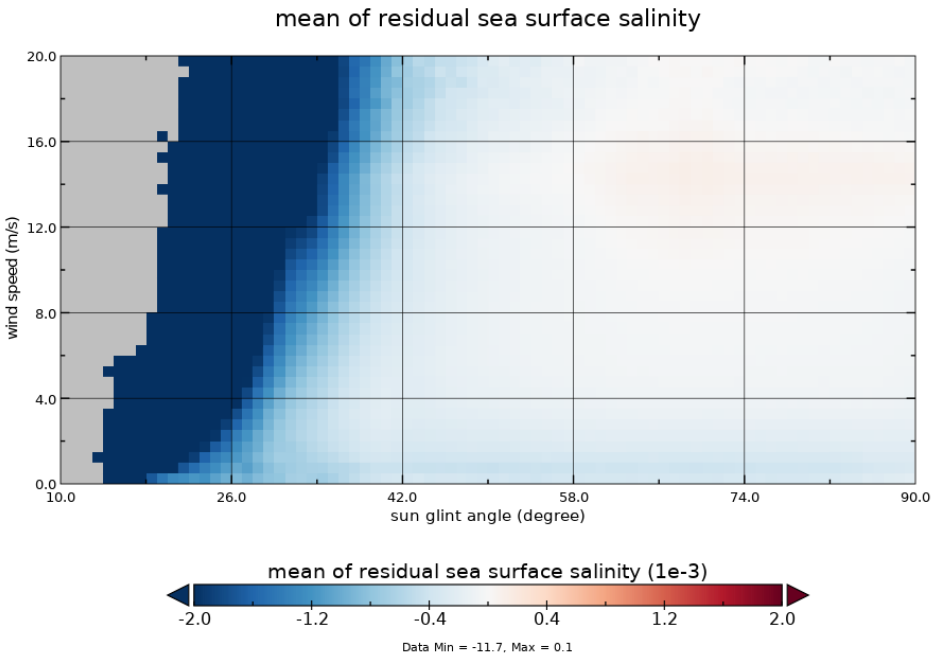

Figure 27: The mean of the residual SSS as a function of sun glint angle and wind speed. Large magnitude errors are clamped for display purposes. The grey shaded area contains no data.

For Version 4, we defined a revised sun glint flag that is a function of both the sun glint angle as well as the wind speed (but not a function of scan angle). The QC flag is set if the sun glint angle is below 50°, and if the wind speed w exceeds a threshold, which is a parameter of sun glint angle g:

$$w > \frac{1}{8000} \cdot (g - 30^{\circ})^4 \qquad (12)$$

With this revised sun glint QC flag applied, the mean of the residual SSS is shown in Figure 29. The discontinuity at the 50° line is removed and no large bias from solar contamination is present.

With the revised sun glint QC flag, the number of valid observations retained is larger than with the previous version of the flag (Figure 30). The mean of the SSS residual is shown in Figure 31 and the root-mean-square (RMS) error is shown in Figure 32. These show that although the number of SMAP measurements retained increases with the revised sun glint QC flag, the error in the additional measurements is similar to non-contaminated cases. This indicates that there is no significant solar contamination in additional measurements.

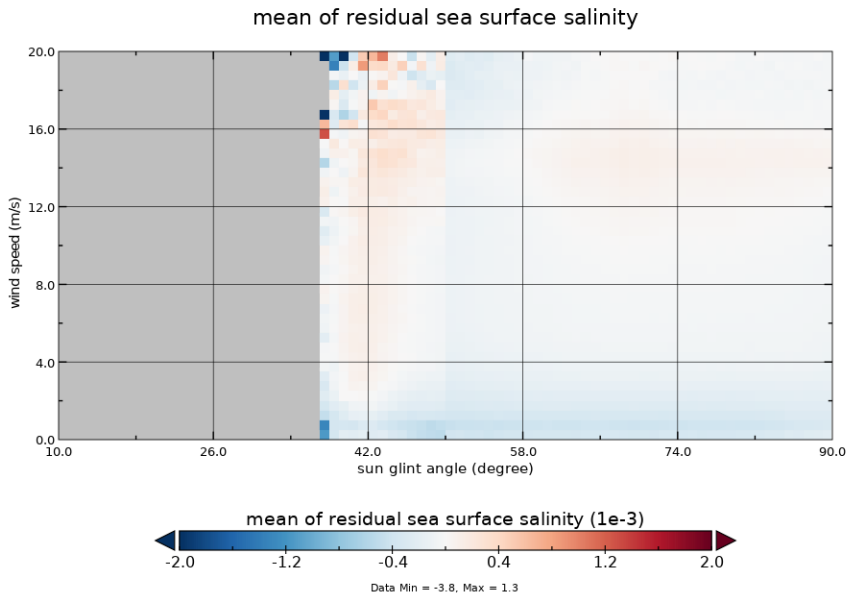

Figure 28: As Figure 27, but the V3 sun glint QC flag is used to mask out data.

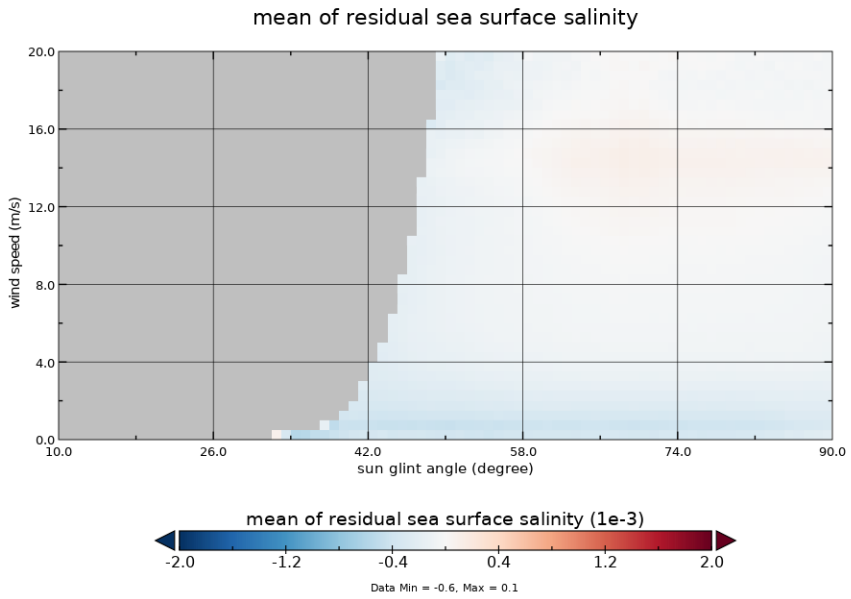

Figure 29: As Figure 27, but with the revised sun glint QC flag for V4.

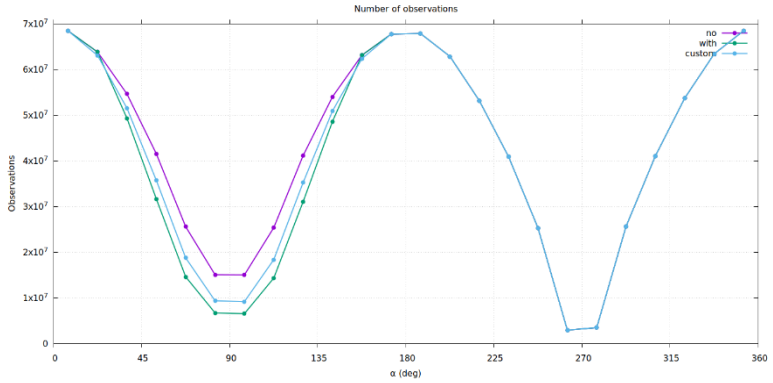

Figure 30: The number of valid observations as a function of scan angle. The three cases are without the sun glint QC flag (purple), with the V3 sun glint QC flag (green), and with the revised V4 sun glint QC flag (blue).

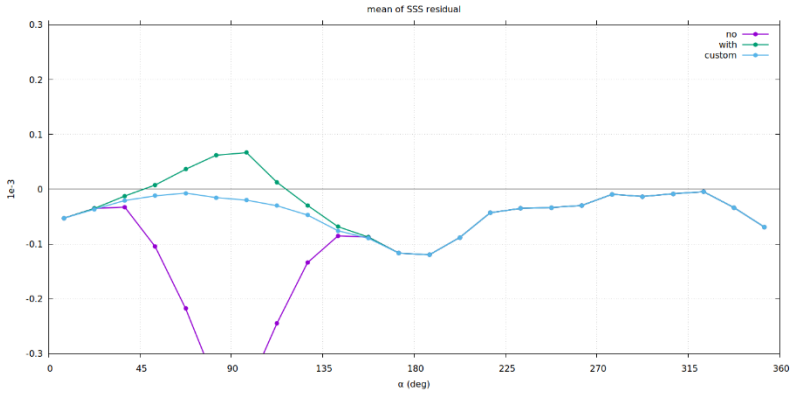

Figure 31: Similar to Figure 30, but the mean of the SSS residual as a function of scan angle for the three cases.

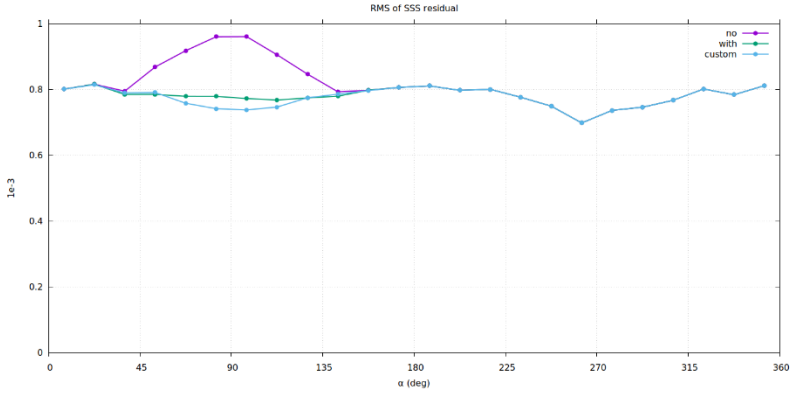

Figure 32: Similar to Figure 30, but the root-mean-square error of the SSS residual as a function of scan angle for the three cases.

5.2.2 Sun Glint Flagging in V6

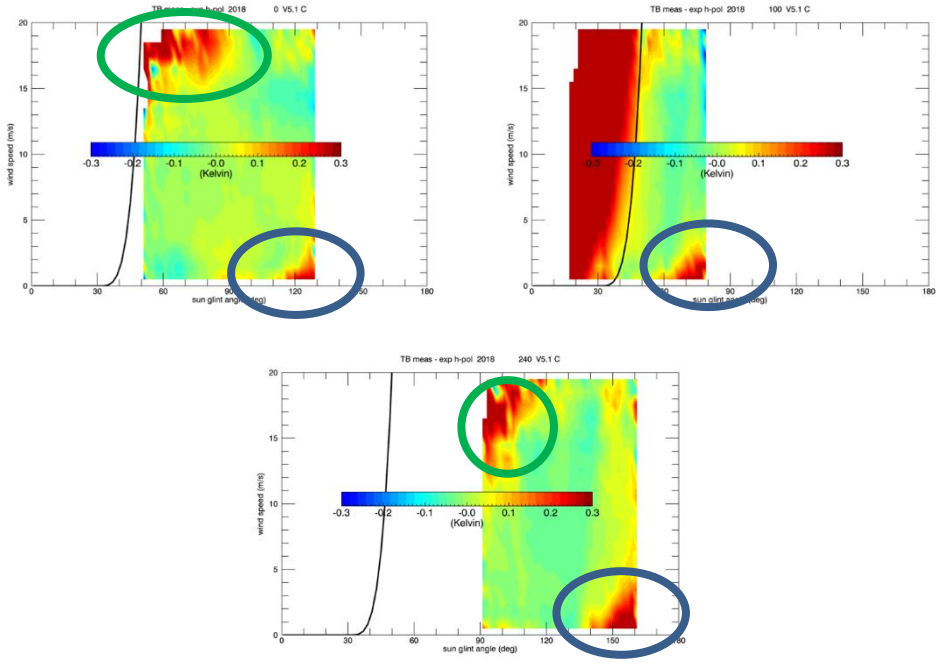

Figure 33. TB measured – expected (h-pol) as function of sun-glint angle (x-axis) and wind speed (y-axis) for various look directions α. Upper left: α=0. Upper right: α=100 deg. Lower center: α=240 deg. The black curve shows the sun glint flag that is used in V5. Observations that lie to the right of the black curve are flagged in V5. The blue ellipses show cases where the sun is reflected into the antenna sidelobes. The green ellipses show cases where the sun is backscattered from the rough ocean surface.

A couple small changes in the sun glint flagging procedure were performed for the V6 release:

1. V5 flags observations if the sun glint angle is less than 30 deg, which also includes negative glint angles. Negative glint angles are defined as cases where the reflected sun ray is eclipsed by the Earth. It is not necessary to flag for this condition, so in V6 the flag is not set for negative glint angles.

2. When looking into the sun (look angle α around 90 deg), small sun glint intruding at high latitudes and low winds is seen in V5. In V6, the sun glint flag is set when the sun glint angle is less than 45 deg, and the wind speed is less than 5 m/s.

3. Small sun glint is seen in V5 at higher sun glint angles and low wind speeds. This is likely caused by the reflected sun intruding into the antenna sidelobes. For V6, a geometrical procedure was developed to flag for that. For each look angle α an angle g_{max} is determined. Then, an elliptical shape is cut out in the (glint angle, wspd) plane around g_{max}. See Figure 34.

4. Small sun glint is seen in V5 at higher wind speeds mainly when looking away from the sun (α around 270 deg). The likely cause is sun that is hitting the main lobe after being backscattered off of very rough surfaces. For V6, a geometrical procedure was developed to flag for that. For

each look angle α an angle h_{min} is determined. Then, an elliptical shape is cut out in the (glint angle, wspd) plane around h_{min}. See Figure 34.

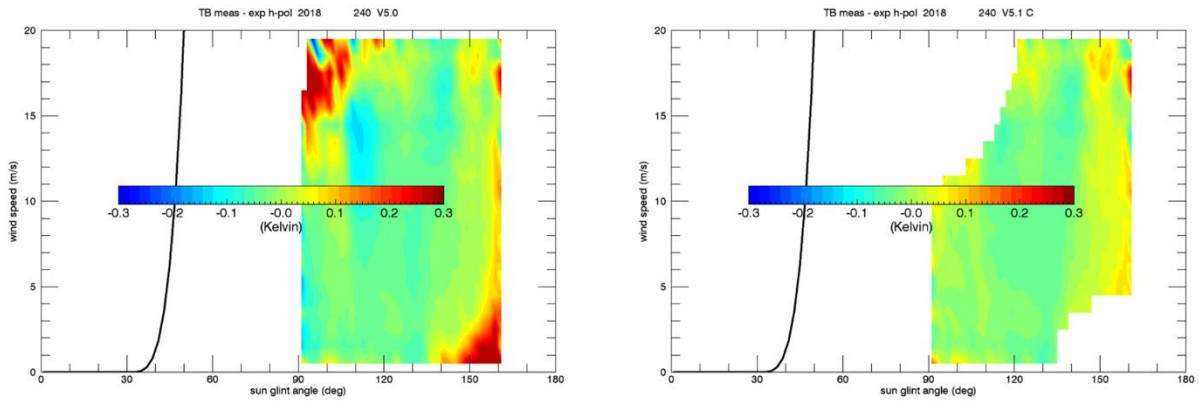

Figure 34. Left: Sun glint flag in V5. Right: Sun glint flag for V6. Elliptical shapes are cut out and flagged.

5.3 Sea-Ice

5.3.1 Ancillary Sea-Ice Products in Releases Prior to Version 5

For the NASA/RSS Aquarius salinity retrieval up to Version 4 and the RSS SMAP salinity retrieval up to and including Version 3, the daily sea-ice mask from NCEP was used as an ancillary field for sea-ice flagging. Brucker et al. 2014 and Dinnat and Brucker (2016) found that the NCEP sea-ice mask is unrealistic in several instances. Consequently, for the Aquarius Version 5 end of mission release, a sea-ice mask from SSMI and AMSR-2 was implemented instead of the NCEP sea-ice mask.

For the SMAP Version 4 release, we switched from NCEP to the sea-ice mask of the RSS Version 8 AMSR-2 ocean suite, which is produced as part of AMSR-2 the daily files (Wentz et al. 2014). This ice mask is more reliable than the NCEP product. However, the AMSR-2 sea-ice mask only contains binary flag values which indicate whether or not sea-ice is present and does not contain any information on the actual sea-ice concentration (SIC) within the SMAP footprint. It was also found that large icebergs near the Antarctic were sometimes not detected and flagged when using the AMSR-2 sea-ice mask, which resulted in erroneous salinity retrievals.

An analysis of other available external ancillary SIC products (OSI-SAF AMSR2, NSIDC CDR) revealed that these products are not reliable for detecting low SIC outside the sea-ice edge. It was discovered that using these products to detect and flag sea-ice in SMAP salinity retrievals frequently resulted in either over- or underflagging of SMAP observations.

5.3.2 Sea-Ice Detection, Masking, and Sidelobe Correction in the SMAP V5 and V6 Releases

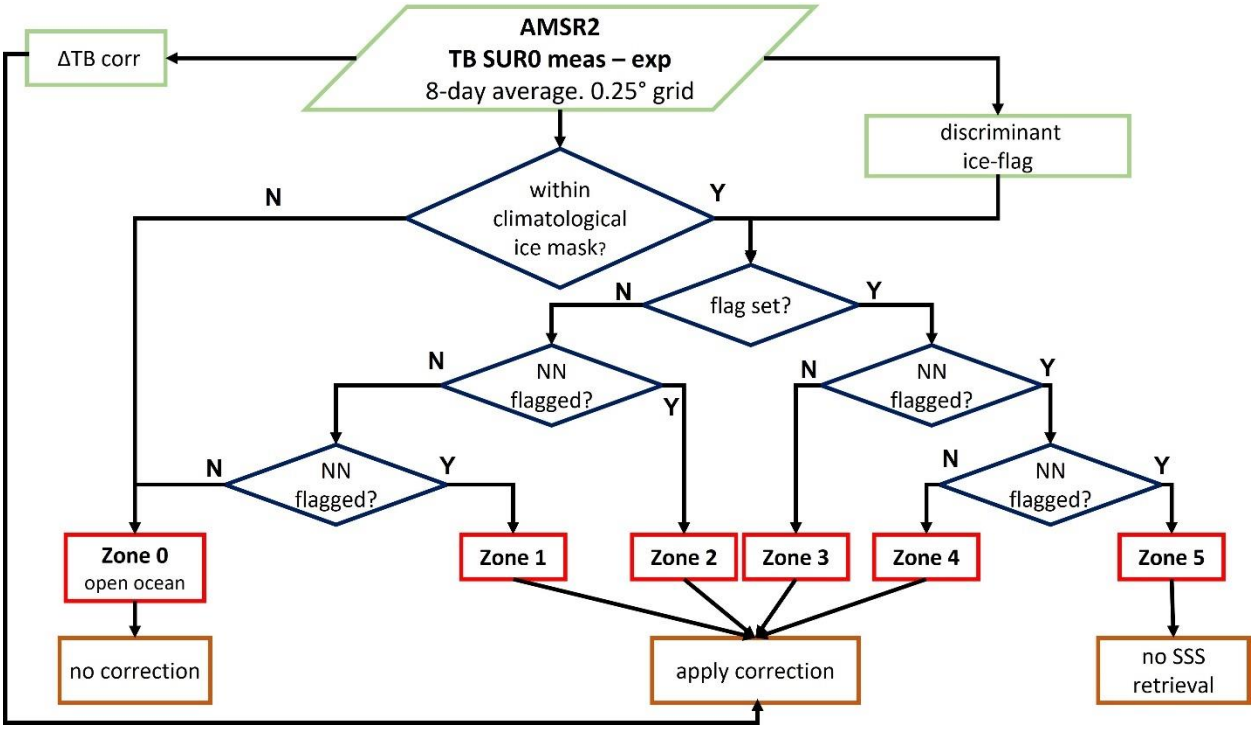

Figure 35: Schematic flow of sea-ice detection and masking in the SMAP V5.0 release based on Meissner and Manaster (2021).

The V5 and V6 releases use the method outlined by Meissner and Manaster (2021) for detecting sea-ice, masking sea-ice contaminated SMAP observations, and performing a side-lobe correction for sea-ice contamination. This method does not use an external sea-ice products but rather ingests 8-day aggregate AMSR-2 TBs. We use 10 AMSR-2 TB channels: both vertical and horizontal polarizations for 6.93, 10.65, 18.7, 23.8, 36.5 GHz. The AMSR-2 7.3 GHz channels are only used for detecting possible RFI in the AMSR-2 C-band frequencies and are not used in the sea-ice detection or correction algorithm. The TOA AMSR-2 TB are turned into specular surface emissivities after removing atmosphere and wind roughness following the steps outlined in 'Method 2' from Meissner and Manaster (2021). In order to do this, we use the same ancillary fields (atmosphere, wind speed, SST) as in the SMAP salinity retrievals (section 3.3).

This method allows for the classification of sea-ice zones (Figure 35, Table 4), which indicate the level of severity of sea-ice contamination in the SMAP observations.

The sidelobe correction $\Delta T_{B,SIC}$, for sea-ice contamination is also derived from the ingested AMSR-2 TB. We derive separate corrections for SMAP V-pol and H-pol channels. The correction values at a given L2 grid cell are the same for fore and aft looks. The value of the correction $\Delta T_{B,SIC}$ is subtracted from the SMAP T_{Bsur0}, which are the specular surface SMAP TB after removing the wind roughness correction. The values of the correction $\Delta T_{B,SIC}$ for each SMAP observation cell are included in the L2C data.

An estimate of the antenna weighted sea-ice fraction g_{ice} can be computed according to:

$$g_{ice} \approx \frac{\Delta T_{B,SIC}}{\left(T_{B,ice} - T_{B,ocean}\right)} \tag{13}$$

We use the V-pol value of $\Delta T_{B,SIC}$ and a typical value of 125 K for the V-pol difference $\left(T_{B,ice} - T_{B,ocean}\right)$ to compute an estimate for g_{ice} , which is recorded in the L2C and L3 files.

Table 4. Overview of sea-ice zones and sea-ice correction (SIC) in the SMAP salinity retrieval algorithm.

sea-ice zone	action	average g_{ice} est (%)	average RMS error after SIC (psu)	average RMS error before SIC (psu)
0 (cold water)	open ocean SSS retrieved. no SIC applied	0.0	2.2	2.2
1	SSS retrieved. SIC applied.	0.2	2.6	3.0
2	SSS retrieved. SIC applied.	0.35	3.1	4.1
3	SSS retrieved. SIC applied.	1.1	5.4	9.7
4	SSS retrieved. SIC applied.	3.8	7.5	25.4
5	no SSS retrieved. no SIC applied.	N/A	N/A	N/A

Table 4 gives the estimated SSS error values for the 40-km L2 product. These values were obtained by comparing SMAP retrieved SSS with HYCOM in the Antarctic using 1 full year of data. The values for zone 0 have been computed for observations that lie within the climatological sea-ice mask and, thus, have cold SST, but are identified as open ocean scenes by the sea-ice detection algorithm.

We provide (1) the climatological sea-ice flag, (2) the RSS AMSR-2 AS-ECV V8.2 8-day aggregate sea-ice flag, and (3) the 8-day aggregate sea-ice flag from Meissner and Manaster (2021) as the variable **anc_sea_ice_flag** in the L2C and 8-day L3 files. The 8-day aggregate RSS AMSR-2 AS-ECV V8.2 sea-ice flag is set, if at least 1 AMSR-2 observation within the time period is flagged as sea-ice by the RSS AMSR-2 AS-ECV V8.2 algorithm.

We note that spatial averaging (40-km to 70-km), averaging fore and aft observations, or temporal averaging in the L3 processing (8-day, monthly) typically does NOT result in significant reduction of errors due to sea-ice contamination.

5.3.3 Exception Handling for Missing AMSR-2 Data

Exceptions in the V5.0/V6.0 sea-ice detection and correction algorithm occur if no AMSR-2 TB observations are present. That typically happens close to the coast or if RFI is detected or suspected in the AMSR-2 TB. Sea-ice close to coast can result in intrusion of both land and sea-ice contamination of the SMAP data, which can neither be handled by the land correction nor the sea-ice correction algorithms. In these cases, no SMAP SSS is retrieved.

There are 2 specific major exception cases:

1. Sea-ice zone 6: The AMSR-2 C-band observations (50-km resolution) are land contaminated or missing. We cannot apply the method outlined in Meissner and Manaster (2021), which requires AMSR-2 C-band TB. We can still check for the RSS AS-ECV V8.2 sea-ice flag, which requires frequencies at X-band and higher. If this sea-ice flag is set, we do not retrieve SMAP SSS and do not apply a SIC to the SMAP TB i.e., bit 3 in the Q/C flag *iqc_flag* is set (section 6).

2. Sea-ice zone 7: The AMSR-2 X-band or higher frequency channels (35-km resolution) are land contaminated or missing. No sea-ice check can be performed based on AMSR-2. If the observation lies within the climatological sea-ice mask, we do not retrieve SMAP SSS and do not apply a SIC to the SMAP TB i.e., bit 16 in the Q/C flag *iqc_flag* is set (section 6).

5.3.4 Sea-Ice Exclusion for Calculating Smoothed Product

The smoothed product *sss_smap* is obtained from the 40-km product *sss_smap_40km* by computing the next-neighbor average at each 0.25^o grid cell. See section 2.10 equation (1). The next-neighbor average normally consists of the center cell plus 8 adjacent cells, but cells are excluded in the case of sea-ice contamination. Specifically, cells are not included if they fall within sea-ice zones 3 or 4.

5.4 Rain

In areas of rain, there is a stratification of the upper ocean layer resulting in fresher salinity right at the ocean surface, measured by SMAP, than at 5-meter depth, measured by ARGO floats or referenced by HYCOM. For details see Boutin et al. 2016. The presence of rain can also cause SMAP salinity retrievals to become less reliable due to possible degraded ancillary wind speed observations or poor atmospheric correction in these areas. Because of these potential issues, we provide ancillary rain rate values from the IMERG product in the SMAP L2C files for basic quality control.

The IMERG rain product (Huffman et al. 2019), available from https://pps.gsfc.nasa.gov/, is a Level 4 merged product for surface rain rates, which is largely based on observations by NASA's Global Precipitation Mission (GPM). It is currently regarded as the best available merged rain product by the scientific community. It is available for the whole SMAP operational period. We are using the Version 6 30-minute 0.1^o product. The IMERG rain rate R_{IMERG} is resampled from

its 0.1° spatial resolution to the 40-km SMAP resolution. At each cell of the SMAP 0.25° fixed Earth grid, we compute an average IMERG rain rate by integrating over an approximate SMAP antenna gain. This approximate antenna gain is a circular Gaussian function with a half-power width of 40-km in both spatial dimensions.

Note that the **value of the IMERG rain rate is not directly used in the Version 5 or Version 6 salinity retrieval.** Also note that only rain-flagged values are included in the ocean-target calibration (Section 4.7) and for producing only rain flagged Level 3 data (Section 7).

The SMAP V5 and V6 salinity retrieval algorithms use cloud water density profiles from the ¼ deg 6-houry NCEP GDAS product. The cloud water mixing ratio in the NCEP profiles is transformed into liquid cloud water density, from which the cloud water absorption at L-band is calculated using the dielectric constant for pure (cloud) water by Meissner and Wentz (2004) and the atmospheric temperature profile.

6 QUALITY CONTROL (Q/C) FLAGS

The V6 salinity retrieval algorithm produces the following Q/C flags (note that these are the same flags used in V5):

Table 5: 32- bit Level 2 Q/C flags in the SMAP V6.0 release.

bit	Q/C flag if bit is set	SSS value and expected level of degradation
0	**no valid radiometer observation in cell**	SSS value set to missing/invalid
1	**problem with OI:** parameter *wt_sum* not normalized to 1	SSS value set to missing/invalid
2	**strong land contamination:** gain weighted land fraction *gland* exceeds 0.1 or land fraction in 3-dB footprint *fland* exceeds 0.1	SSS value set to missing/invalid
3	**strong sea ice contamination:** observation falls within sea-ice zone 5 or the observation falls within sea-ice zone 6 (close to land or no AMSR-2 C-band TB available) and the sea-ice flag from RSS AS-ECV V8.2 is set. See section 5.3).	SSS value set to missing/invalid
4	**MLE in SSS retrieval has not converged**	SSS value set to missing/invalid
5	**sunglint:** see section 5.2	SSS retrieved very strong degradation not included in averaging for the 70-km smoothed product
6	**moonglint:** moonglint angle *mongl*t less than 15°	SSS retrieved moderate – strong degradation not included in averaging for the 70-km smoothed product
7	**high reflected galaxy:** 1st component *ta_gal_ref(1, …)/2* [=(V+H)/2] exceeds 2.0K.	SSS retrieved moderate – strong degradation not included in averaging for the 70-km smoothed product
8	**moderate land contamination:** gain weighted land fraction *gland* exceeds 0.04 or land fraction in 3-dB footprint *fland* exceeds 0.005	SSS retrieved moderate -strong degradation not included in averaging for the 70-km smoothed product
9	**moderate sea ice contamination:** observation falls within sea-ice zones 3 or 4	SSS retrieved strong degradation not included in averaging for the 70-km smoothed product
10	**high residual of MLE in SSS retrieval algo:** variable *tb_consistency* exceeds 1.0 K	SSS retrieved moderate – strong degradation not included in averaging for the 70-km smoothed product
11	**low SST:** *surtep - 273.15* below 5°C	SSS retrieved moderate – strong degradation
12	**high wind speed:** *winspd* exceeds 15 m/s	SSS retrieved moderate degradation
13	**light land contamination** gain weighted land fraction *gland* exceeds 0.001	SSS retrieved light degradation

14	**light sea-ice contamination** observation falls within sea-ice zones 1 or 2	SSS retrieved moderate degradation
15	**rain flag:** IMERG rain-rate (resampled to 40-km SMAP foot-print) exceeds 0.1 mm/h.	SSS retrieved possible light degradation due to degraded wind speed or poor atmospheric correction. Validation of SMAP versus ARGO/HYCOM might result in error due to SSS stratification within the upper ocean layer
16	**no sea-ice check possible** No AMSR-2 TB in X-band and/or higher channels is available, because of either missing data, too close to land, or RFI (sea-ice zone 7) and the observation falls within the climatological sea-ice mask. See section 5.3.3.	SSS value set to missing/invalid
17 - 31	sparse	

7 LEVEL 3 PROCESSING

Both the 40-km (*sss_smap_40km*) and the *sss_smap* (smoothed to approximately 70km) L2C salinity products are averaged into Level 3 data products. The L3 grids are regular 0.25° latitude/longitude Earth grids created by averaging all valid L2C observations within each grid cell, as described in the following. First, fore and aft looks are averaged together. Then, we produce a running 8-day average L3 file and a monthly average L3 file. For an 8-day running average that is centered on a given day of the year (*DOY*) we average all valid observations within +/- 3.5 days of said *DOY*. For example, the L3 file for January 15 is created by averaging all valid L2 observations that fall between 12UTC January 11 and 12UTC January 19. The reason for providing 8-day averages rather than weekly averages is that SMAP has an exact 8-day repeat cycle. For the monthly average files, we average all valid data within the corresponding calendar month. **The L3 processing only involves time averaging of the L2C data. No additional spatial smoothing of the L2C data is done in the L3 processing.**

During the gridding for both the 8-day running averages and the monthly averages, we apply the following Q/C **in addition to the L2C Q/C checks**. The L3 processing discards observations, if:

1. The sun glint flag (bit 5 in L2 Q/C flag Table 5) is set. See section 5.2.
2. The moon glint angle is less than 15° (bit 6 in L2 Q/C flag Table 5 is set).
3. The v/h-pol average of the reflected galactic radiation exceeds 2.0 K (bit 7 in L2 Q/C flag Table 5 is set).
4. The TB consistency, which is defined as the $\sqrt{\chi^2}$ of the MLE in the salinity retrieval algorithm, exceeds 1.0 K (bit 10 in L2 Q/C flag Table 5 is set).
5. The wind speed exceeds 20 m/s.

The L3 files contain the number of observations in each grid cell as well as averaged values of salinity, g_{land}, f_{land}, g_{ice}, and the ancillary SST in each grid cell.

Browsing images for both 8-day and monthly averages are available on the RSS website (http://www.remss.com/missions/smap/).

In V5 and V6, we also produce rain-filtered (RF) 8-day and monthly smoothed (70-km) L3 products. In doing so, we discard data if the IMERG rain rate (Sections 3.3 and 5.4) exceeds 0.1 mm/h (bit 15 in Table 5 is set). The RF products are included as additional fields in their corresponding L3 files. In prior releases, the RF products had been distributed as separate files. The purpose of the rain filtering is to eliminate mismatch between SMAP SSS, measured at the surface, and in-situ observations (ARGO floats) or HYCOM, which generally observe salinity at depths of about 5-meters. This mismatch occurs due to salinity stratification of the upper ocean layer in rain (Boutin et al. 2016). Therefore, the RF products are better suited when comparing or validating SMAP SSS observations with ARGO floats or HYCOM.

8 FORMAL UNCERTAINTY ESTIMATES

Table 6. Error sources and propagation for the SMAP V6.0 formal uncertainty estimates.
Random propagation (ran). Systematic propagation (sys). These are the same error sources and propagation methods used in SMAP V5.0.

error source		method of estimation	propagation		
			spatial smoothing	fore-aft	time average
1	wind speed (random)	CCMP wind speed validation: Std.Dev. of CCMP – buoy wind speed. The error depends on CCMP wind speed and the number of satellite observations in the CCMP analysis. Mears et al. 2019.	sys	sys	ran
2	NEDT v-pol	Instrument parameter. We assume an ocean NEDT of 0.9 K and a noise reduction factor of 0.4 in the OI.	ran	ran	ran
3	NEDT h-pol	Instrument parameter. We assume an ocean NEDT of 0.9 K and a noise reduction factor of 0.4 in the OI.	ran	ran	ran
4	SST	SST uncertainty values provided by CMC.	sys	sys	ran
5	wind direction	CCMP wind direction validation: Std.Dev. of CCMP – buoy wind direction. The error depends on the number of satellite observations in the CCMP analysis. Mears et al. 2019.	ran	ran	ran
6	reflected galaxy	We allocate 5% of the reflected galaxy as residual error in the 40-km L2C product.	ran	ran	ran
7	land contamination	Analysis of TB (meas – exp) in coastal areas. We allocate 50% of the derived land correction as residual error in the 40-km L2C product.	ran	sys	sys
8	sea-ice contamination	Analysis of TB (meas – exp) near Antarctica.	sys	sys	sys
9	wind speed (systematic)	CCMP wind speed validation: Bias of CCMP – buoy wind speed. The error depends on CCMP wind speed and the number of satellite observations in the CCMP analysis. Mears et al. 2019.	sys	sys	sys

SMAP V5 and V6 provide formal uncertainty estimates for all salinity retrievals, both at L2C and L3, for the 40-km product as well as the 70-km smoothed product.

Estimating the formal uncertainty follows the method established for Aquarius (Meissner 2015; Meissner et al. 2017, 2018). It consists of the following steps:

1. Identifying all parameters λ in the retrieval algorithm, whose uncertainty results in a sizeable error for the retrieved SSS.

2. Making a quantitative estimate for the uncertainty Δλ.

3. Running the salinity algorithm by perturbing the input for λ and then computing the derivative

$$\frac{\partial SSS}{\partial \lambda} \approx \frac{SSS(\lambda + \Delta\lambda) - SSS(\lambda - \Delta\lambda)}{2\Delta\lambda}.$$

4. Calculating the uncertainty estimate for SSS for an error in λ. This uncertainty estimate is given by: $\Delta SSS_{\lambda} = \frac{\partial SSS}{\partial \lambda} \cdot \Delta\lambda$.

5. Obtaining the total formal uncertainty. This is calculated as the root sum squared of the single errors in each parameter.

It is necessary to assess and specify how each error source propagates when performing spatial averaging (smoothing from 40-km to 70-km), averaging fore and aft observations (during L3 averaging), and performing temporal averaging to create the L3 products (8-day or monthly). Random error propagation involves an error reduction by $1/\sqrt{N}$, where *N* is the number of observations that go into the average. For systematic error propagation there is no error reduction when averaging.

Table 6 shows the error sources on the SMAP V6.0 release, how they are assessed, and how they propagate.

9 PERFORMANCE ESTIMATE AND VALIDATION

See the presentation by Kao et al 2023, which contains the extensive validation analysis for V5.3 that was performed by the Earth and Space Research (ESR) team.

10 NEAR REAL TIME (NRT) SALINITY DATA

SMAP salinity quick-look Level 2C files are provided in near-real time (NRT) with a latency of approximately 5 hours.

The major differences between the SMAP NRT product and the SMAP Final product are:

1. We ingest the NRT version of the L1B SMAP antenna temperatures, which are publicly available from NSIDC at https://nsidc.org/data/spl1btb_nrt/versions/105.

The NRT version of the L1B data uses pre-computed S/C ephemeris data, which allows for a faster data down-link.

2. For the ancillary wind speed and direction input, we use the latest 6-hourly 0.25^{o} wind speed and direction. There is no time interpolation done. The latency of the ancillary wind fields is the determining factor for the latency of the NRT salinity. Using the NCEP wind fields instead of the CCMP wind fields allows to cut the latency of the NRT salinity to a few hours. The tradeoff is the accuracy of the salinity product: The typical RMS of the L2C salinity increases from about 0.6 psu (FINAL SSS product) to about 0.9 psu (NRT SSS product) due to the degraded accuracy of the input wind field.

3. For the ancillary SST input, we use the CMC SST from 2 days earlier.

4. For the sea-ice flag (section 5.3), we use the sea-ice mask of the 3-day aggregate RSS AMSR-2 Air-Sea Essential Climate Variables (AS-ECVs) dataset (https://www.remss.com/missions/amsr/) from 2-days earlier.

5. No correction for sea-ice contamination (section 5.3) is performed. It is recommended to only use SMAP data that are classified to be within sea-ice zone 0.

11 SUPPORTING DOCUMENTS AND PUBLICATIONS

All supporting documents are available at: https://data.remss.com/smap/SSS/V06.0/documents/.

Kao, H.-Y, J. Anderson, J. Schanze, S. Howard and O. Melnichenko, SVDS for SMAP RSS V5.3 and comparisons with SMAP RSS V5.0. Earth and Space Research, 2023.

Meissner, T., F. Wentz, and L. Ricciardulli, 2014: The emission and scattering of L-band microwave radiation from rough ocean surfaces and wind speed measurements from Aquarius, J. Geophys. Res. Oceans, vol. 119, http://doi.org/10.1002/2014JC009837.

Meissner, T., 2015: Assessment of Uncertainties in Aquarius Salinity Retrievals, RSS Technical Report 061015. Available online at https://data.remss.com/smap/SSS/V05.0/documents/.

Meissner, T., F. Wentz F. and D. M. Le Vine, 2017, Aquarius Salinity Retrieval Algorithm Theoretical Basis Document (ATBD), End of Mission Version; RSS Technical Report 120117; 1 December 1, 2017. Available online at https://images.remss.com/papers/tech_reports/2017/Meissner_AQ_ATBD_EOM_final.pdf.

Meissner, T, F.J. Wentz, and D.M. Le Vine, 2018, The Salinity Retrieval Algorithms for the NASA Aquarius Version 5 and SMAP Version 3 Releases, Remote Sensing 10, 1121, https://doi.org/10.3390/rs10071121.

Meissner, T., and A. Manaster, 2021, SMAP Salinity Retrievals near the Sea-Ice Edge Using Multi-Channel AMSR2 Brightness Temperatures. *Remote Sens.* vol. 13, pp. 5120. https://doi.org/10.3390/rs13245120.

12 REFERENCES

Atlas, R., R. N. Hoffman, J. Ardizzone, S. M. Leidner, J. C. Jusem, D. K. Smith, D. Gombos, 2011: A cross-calibrated, multiplatform ocean surface wind velocity product for meteorological and oceanographic applications. Bull. Amer. Meteor. Soc., 92, 157-174. doi: 10.1175/2010BAMS2946.1

Boutin, J. et al., Satellite and In Situ Salinity: Understanding Near-Surface Stratification and Subfootprint Variability. Bulletin of the American Meteorological Society, 97, 1391–1407, doi: 10.1175/BAMS-D-15-00032.1.

Brucker, L., E. Dinnat, and L. Koenig, 2014, Weekly gridded Aquarius L-band radiometer/scatterometer observations and salinity retrievals over the polar regions-Part 2: Initial product analysis, Cryosphere, 8(3), 915–930, doi:10.5194/tc-8-915-2014.

Dinnat, E. and L. Brucker, 2016, Improved Sea Ice Fraction Characterization for L-Band Observations by the Aquarius Radiometers, IEEE Transactions on Geoscience and Remote Sensing, doi:10.1109/TGRS.2016.2622011.

Huffman, G. et al., 2019, NASA Global Precipitation Measurement (GPM) Integrated Multi-satellitE Retrievals for GPM (IMERG), Version 6, NASA, Available online at https://pmm.nasa.gov/sites/default/files/document_files/IMERG_V06_release_notes_190503.pdf.

Kao, H.-Y., G. Lagerloef, T. Lee, O. Melnichenko, T. Meissner and P. Hacker, 2018, Assessment of Aquarius Sea Surface Salinity, Remote Sens. 10(9), https://doi.org/10.3390/rs10091341.

Lee, T., 2016, Consistency of Aquarius sea surface salinity with Argo products on various spatial and temporal scales, Geophys. Res. Lett., vol. 43(8), pp 3857-3864, https://doi.org/10.1002/2016GL068822.

Liebe, H., P. Rosenkranz and G. Hufford, 1992, Atmospheric 60-GHz oxygen spectrum: New laboratory measurements and line parameters, J. Quant. Spectrosc. Radiat. Transfer, 48, 629–643, doi: 10.1016/0022-4073(92)90127-P.

Mears, C. et al. 2018: Remote Sensing Systems Cross-Calibrated Multi-Platform (CCMP) 6-hourly ocean vector wind analysis product on 0.25 deg grid, Version 2.0. Remote Sensing Systems, Santa Rosa, CA. Available online at www.remss.com/measurements/ccmp.

Mears, C. A., Scott, J., Wentz, F. J., Ricciardulli, L., Leidner, S. M., Hoffman, R., & Atlas, R., 2019: A Near-Real-Time Version of the Cross-Calibrated Multiplatform (CCMP) Ocean Surface Wind Velocity Data Set. Journal of Geophysical Research: Oceans, 124, 6997– 7010. https://doi.org/10.1029/2019JC015367

Meissner, T., and F. Wentz, 2004, The complex dielectric constant of pure and sea water from micro-wave satellite observations, IEEE TGRS, vol. 42(9), pp 1836.

Meissner, T. and F. Wentz, 2012, The emissivity of the ocean surface between 6 and 90 GHz over a large range of wind speeds and Earth incidence angles, IEEE TGRS, 2012, 50(8), 3004–3026, doi: 10.1109/TGRS.2011.2179662.

Meissner, T., F. Wentz, and L. Ricciardulli, 2014: The emission and scattering of L-band microwave radiation from rough ocean surfaces and wind speed measurements from Aquarius, J. Geophys. Res. Oceans, vol. 119, doi: 10.1002/2014JC009837.

Meissner, T., F. Wentz F. and D. M. Le Vine, 2017, Aquarius Salinity Retrieval Algorithm Theoretical Basis Document (ATBD), End of Mission Version; RSS Technical Report 120117; 1 December 1, 2017. Available online at https://images.remss.com/papers/tech_reports/2017/Meissner_AQ_ATBD_EOM_final.pdf.

Meissner, T, F.J. Wentz, and D.M. Le Vine, 2018, The Salinity Retrieval Algorithms for the NASA Aquarius Version 5 and SMAP Version 3 Releases, Remote Sensing 10, 1121, doi:10.3390/rs10071121.

Meissner, T., and A. Manaster, SMAP Salinity Retrievals near the Sea-Ice Edge Using Multi-Channel AMSR2 Brightness Temperatures. *Remote Sens.* 2021, vol. 13, pp. 5120. https://doi.org/10.3390/rs13245120.

Piepmeier, J. et al., 2023: SMAP Calibrated, Time-Ordered Brightness Temperatures L1B_TB Data Product, Algorithm Theoretical Basis Document (ATBD), https://smap.jpl.nasa.gov/documents/.

Piepmeier J. et al., 2023. SMAP L1B SMAP L1B Radiometer Half-Orbit Time-Ordered Brightness Temperatures, Version 6. Boulder, Colorado USA. NASA National Snow and Ice Data Center Distributed Active Archive Center. https://doi.org/10.5067/GWYQTF307Y9Y.

Poe, G., 1990, Optimum interpolation of imaging microwave radiometer data, IEEE Trans. Geosci. Remote Sens., vol. 28, no. 5, pp. 800-810.

Stogryn, A., 1978, Estimates of brightness temperatures from scanning radiometer data, IEEE Trans. Antennas Propag. vol. AP-26, no. 5, pp. 720 – 726.

Vazquez-Cuervo, J. et al., 2019, Using Saildrones to Validate Satellite-Derived Sea Surface Salinity and Sea Surface Temperature along the California/Baja Coast, Remote Sensing, https://doi.org/10.3390/rs11171964.

Wentz et al., 2021, Remote Sensing Systems GCOM-W1 AMSR-2 AS-ECV on 0.25 deg grid, Version 8.2, Available from www.remss.com/amsr/.

Wentz, F., and T. Meissner, 2016: Atmospheric absorption model for dry air and water vapor at microwave frequencies below 100GHz derived from spaceborne radiometer observations, Radio Science, vol. 51, doi:10.1002/2015RS005858.

13 DATA FORMAT SPECIFICATION

13.1 Level 2C Final

13.1.1 Paths and Filenames

- **Pathname:** https://data.remss.com/smap/SSS/V06.0/FINAL/L2C//yyyy/mm/...
  yyyy = 4-digit year, mm = 2-digit month.

- **Filename:** *RSS_SMAP_SSS_L2C_rnnnnn_yyyymmddThhmiss_yyyyddd_FNL_V06.0.nc*.
  nnnnn = 5-digit orbit (rev) #, yyyy = 4-digit year, mm = 2-digit month, dd = 2-digit day of month, hh=2-digit hour of day (UTC), mi = 2-digit minute of hour (UTC), ss = 2-digit second of minute (UTC), doy 3-digit day of year. The time stamp refers to the start time of the orbit.

13.1.2 Global Attributes

- **orbit_number** (4-byte integer): orbit (rev) #.

- **start_time_sec2000** (8-byte real): seconds of first valid record in this rev since 2000-01-01 00:00:00 UTC.

- **start_time_year, start_time_month, start_time_day_of_month, start_time_day_year** (4-byte integer): year, month, day of month, day of year of first valid record in this rev.

- **start_time_sec_of_day** (8-byte real): seconds of day of first valid record in this rev.

- **end_time_sec2000** (8-byte real): seconds of last valid record in this rev since 2000-01-01 00:00:00 UTC.

- **end_time_year, end_time_month, end_time_day_of_month, end_time_day_year** (4-byte integer): year, month, day of month, day of year of last valid record in this rev.

- **end_time_sec_of_day** (8-byte real): seconds of day of last valid record in this rev.

- **emissivity_reflector_vpol, emissivity_reflector_hpol** (4-byte real): ε_{ant} (Section 4.3).

- **A_ij** (4-byte real): APC matrix element (i, j) where the indices i, j run over the Stokes vector I, Q, S3, S4 (Section 4.6).

- **ta_ocean_ave_vpol, ta_ocean_ave_hpol** (4-byte real): average ta over open ocean for this rev (Section 4.7).

- **ta_bias_ocean_vpol, ta_bias_ocean_hpol, ta_bias_ocean_S3, ta_bias_ocean_S4** (4-byte real): TA biases= TA measured – expected over the open ocean (Section 4.7). The computation of TA expected is based on the HY-COM reference SSS. The computation of TA expected for the 3rd Stokes parameter (S3) is based on ancillary TEC maps from IGS (Table 2).

13.1.3 Gridding and Dimensions

The L2C files contain SMAP observations that were optimum interpolated onto a fixed 0.25° x 0.25° Earth grid.

The grid (x, y) dimensions are:

- **xdim_grid=1560**, which corresponds to 360° longitude plus 30° in order to accommodate the whole swath.

- **ydim_grid =720**, which corresponds to 180° latitude.

Though the grid cell indices are related to longitude and latitude, the variables cellon and cellat (Section 13.1.4) should be used to identify the location.

- **look** = 2 (1 = for look, 2= aft look) defines the look direction of the variable. If the variable does not depend on look direction, then this dimension is omitted.

- **polarization_2** = 2, **polarization_3** = 3, **polarization_4** = 4 specifies the polarization of the variable fields. Note that for some variables the Stokes polarization basis (I, Q, S3, S4) is used, whereas for other variables the modified Stokes polarization basis (V, H, S3, S4) is used. See section 13.1.4.

- **uncertainty_components** = 9 specifies the 9 components that go into the formal uncertainty estimate. See section 8.

- **iceflag_components** = 3 specifies the 3 components of the ancillary sea-ice indicator. Component 1 = climatological sea-ice mask including iceberg alley near Antarctica. Component 2 = 8-day aggregate sea-ice flag from RSS ASMR-2 AS-ECV V8.2. Component 3= 8-day aggregate sea-ice flag from Meissner and Manaster (2021).

Any grid cell for with one of the bits 0 – 1 set has invalid entries and none of the variable fields should be used. Any grid cells with one of the bits 2 – 3 set has no valid salinity retrieval.

13.1.4 Variables

All variable values refer to the average of the OI in the grid cell.

- **time** (8-byte float, array size = [look, xdim_grid, ydim_grid]): seconds of observation since 2000-01-01 00:00:00 UTC.

- **cellat** (4-byte float, array size = [look, xdim_grid, ydim_grid]): geodetic latitude. range: [90°S, 90°N].

- **cellon** (4-byte float, array size = [look, xdim_grid, ydim_grid]): longitude. range: [0°, 360°].

- **eia** (4-byte float, array size = [look, xdim_grid, ydim_grid]): boresight Earth incidence angle. range: [0°, 90°]

- **eaa** (4-byte float, array size = [look, xdim_grid, ydim_grid]): boresight Earth azimuth angle. range: [0°, 360°].

- **zang** (4-byte float, array size = [look, xdim_grid, ydim_grid]): orbital position angle of S/C. range: [0°, 360°]. It is defined as: $zang = \arctan \frac{\left(\hat{R}_{S/C} \cdot \hat{z}\right)}{\left(\hat{V}_{S/C} \cdot \hat{z}\right)} + 90^{\circ}$. $\hat{z}$ is the z-unit vector in the Earth centered inertial system (ECI). $\hat{R}_{S/C}$ is the S/C location unit vector in the ECI system. $\hat{V}_{S/C}$ is the S/C velocity unit vector in the ECI system. 0° is S, 90° is equator crossing in the ascending swath, 180° is N, 270° is equator crossing in the descending swath, 360° is S.

- **alpha** (4-byte float, array size = [look, xdim_grid, ydim_grid]): scan angle. range: [0°, 360°]. 0° is forward, 90° is left of forward, 180° is aft, 270° is right of forward, 360° is forward.

- **pra** (4-byte float, array size = [look, xdim_grid, ydim_grid]): polarization basis rotation angle (geometrical part), which is the angle between polarization basis of S/C and polarization basis on the Earth. range: [-90^o, +90^o].

- **sunglt** (4-byte float, array size = [look, xdim_grid, ydim_grid]): sun glint angle. range: [-180^o, +180^o]. It is the angle between specular reflection of boresight and the ray to the sun. A negative value means that the ray to the sun is piercing the Earth.

- **monglt** (4-byte float, array size = [look, xdim_grid, ydim_grid]): moon glint angle. range: [-180^o, +180^o]. It is the angle between specular reflection of boresight and the ray to the moon.

- **gallat** (4-byte float, array size = [look, xdim_grid, ydim_grid]): polar angle of specular reflection ray from boresight in ECI J2000 system (Earth centered inertial system of year 2000). range: [-90^o, +90^o].

- **gallon** (4-byte float, array size = [look, xdim_grid, ydim_grid]): azimuthal angle of specular reflection ray from boresight in ECI J2000 system (Earth centered inertial system of year 2000). range: [0^o, +360^o].

- **sun_beta** (4-byte float, array size = [look, xdim_grid, ydim_grid]): sun zenith angle in S/C coordinate system. [0^o, +180^o].

- **sun_alpha** (4-byte float, array size = [look, xdim_grid, ydim_grid]): sun azimuth angle in S/C coordinate system. [0^o, +360^o].

- **gland** (4-byte float, array size = [look, xdim_grid, ydim_grid]): land fraction weighted by antenna gain pattern. range: [0.0, 1.0].

- **fland** (4-byte float, array size = [look, xdim_grid, ydim_grid]): land fraction within footprint. range: [0.0, 1.0].

- **gice_est** (4-byte float, array size = [xdim_grid, ydim_grid]): sea ice fraction weighted by antenna gain pattern. range: [0.0, 1.0]. See section 5.3.2.

- **surtep** (4-byte float, array size = [xdim_grid, ydim_grid]): ancillary sea surface temperature from CMC. Units: Kelvin.

- **winspd** (4-byte float, array size = [xdim_grid, ydim_grid]): ancillary sea surface wind speed from CCMP. see Section 4.2.1. Units: m/s.

- **windir** (4-byte float, array size = [xdim_grid, ydim_grid]): ancillary wind direction relative to N from CCMP. see section 4.2.1. meteorological convention. 0^o: wind coming out of N, +90^o: wind coming out of E, etc. range: [0^o, +360^o].

- **tran** (4-byte float, array size = [xdim_grid, ydim_grid]): total atmospheric transmittance. computed from ancillary NCEP GDAS atmospheric profile fields for pressure, geopotential height, temperature, relative humidity, cloud water mixing ratio. range: [0.0, 1.0].

- **tbup** (4-byte float, array size = [xdim_grid, ydim_grid]): atmospheric upwelling brightness temperature. computed from ancillary NCEP GDAS atmospheric profile fields for pressure, geopotential height, temperature, relative humidity, cloud water mixing ratio. Units: Kelvin.

- **tbdw** (4-byte float, array size = [xdim_grid, ydim_grid]): atmospheric downwelling brightness temperature. computed from ancillary NCEP GDAS atmospheric profile fields for pressure, geopotential height, temperature, relative humidity, cloud water mixing ratio. Units: Kelvin

- **rain** (4-byte float, array size = [xdim_grid, ydim_grid]): IMERG rain rate resampled to SMAP spatial resolution (40 km). see section 5.4. Units: mm/h.

- **solar_flux** (4-byte float, array size = [xdim_grid, ydim_grid]): ancillary mean solar flux from NOAA SWPC. Units: SFU.

- **ta_ant_filtered** (4-byte float, array size = [polarization_4, look, xdim_grid, ydim_grid]): SMAP RFI filtered antenna temperatures. This is the basic input from the SMAP L1B TB files. Units: Kelvin. polarization basis: 1=V, 2=H, 3=S3, 4=S4.

- **ta_ant_unfiltered** (4-byte float, array size = [polarization_4, look, xdim_grid, ydim_grid]): SMAP unfiltered antenna temperatures. Units: Kelvin. polarization basis: 1=V, 2=H, 3=S3, 4=S4.

- **ta_ant_calibrated** (4-byte float, array size = [polarization_4, look, xdim_grid, ydim_grid]): SMAP antenna temperatures after correcting for the emissive antenna (Section 4.3) and after applying the ocean-target calibration (Section 4.7). Units: Kelvin. polarization basis: 1=V, 2=H, 3=S3, 4=S4.

- **ta_earth** (4-byte float, array size = [polarization_4, look, xdim_grid, ydim_grid]): SMAP antenna temperatures after correcting for celestial intrusions: cold space (spillover), galaxy (direct and reflected), sun (direct and reflected) , moon (reflected). Units: Kelvin. polarization basis: 1=V, 2=H, 3=S3, 4=S4.

- **tb_toi** (4-byte float, array size = [polarization_4, look, xdim_grid, ydim_grid]): SMAP top of the ionosphere brightness temperatures. Units: Kelvin. polarization basis: 1=V, 2=H, 3=S3, 4=S4.

- **tb_toa** (4-byte float, array size = [polarization_4, look, xdim_grid, ydim_grid]): SMAP top of the atmosphere brightness temperatures (before applying land correction). Units: Kelvin. polarization basis: 1=V, 2=H, 3=S3, 4=S4.

- **tb_toa_lc** (4-byte float, array size = [polarization_4, look, xdim_grid, ydim_grid]): SMAP top of the atmosphere brightness temperatures after applying land correction (section 5.1). Units: Kelvin. polarization basis: 1=V, 2=H, 3=S3, 4=S4.

- **dtb_land_correction** (4-byte float, array size = [polarization_2, look, xdim_grid, ydim_grid]): SMAP sidelobe correction for land intrusion (See section 5.1). Units: Kelvin. polarization basis: 1=V, 2=H.

- **dtb_sea_ice_correction** (4-byte float, array size = [polarization_2, look, xdim_grid, ydim_grid]): SMAP sidelobe correction for sea-ice intrusion (See section5.3). Units: Kelvin. polarization basis: 1=V, 2=H.

- **tb_sur** (4-byte float, array size = [polarization_4, look, xdim_grid, ydim_grid]): SMAP brightness temperature at rough ocean surface (before applying surface roughness correction, section 4.2). Units: Kelvin. polarization basis: 1=V, 2=H, 3=S3, 4=S4.

- **tb_sur0** (4-byte float, array size = [polarization_4, look, xdim_grid, ydim_grid]): SMAP brightness temperature referenced to flat ocean surface (after applying surface roughness correction, section 4.2 but without applying the sea-ice correction). Units: Kelvin. polarization basis: 1=V, 2=H, 3=S3, 4=S4.

- **tb_sur0_sic** (4-byte float, array size = [polarization_4, look, xdim_grid, ydim_grid]): SMAP brightness temperature referenced to flat ocean surface (after applying surface roughness correction, section 4.2, and after applying the sea-ice correction, section 5.3). Units: Kelvin. polarization basis: 1=V, 2=H, 3=S3, 4=S4.

- **temp_ant** (4-byte float, array size = [polarization_2, look, xdim_grid, ydim_grid]): physical temperature of the SMAP mesh antenna from JPL thermal model $T_{phys,ant}$ (section 4.3). This value is included in SMAP L1B TB files. Units: Kelvin. polarization basis: 1=V, 2=H.

- **dtemp_ant** (4-byte float, array size = [polarization_2, look, xdim_grid, ydim_grid]): empirical correction $\Delta T_{phys,ant}$ to the physical temperature of the SMAP mesh antenna (section 4.3). Units: Kelvin. polarization basis: 1=V, 2=H.

- **ta_sun_dir** (4-byte float, array size = [polarization_3, look, xdim_grid, ydim_grid]): TA of direct sun intrusion. Units: Kelvin. polarization basis: 1=I, 2=Q, 3=S3.

- **ta_sun_ref** (4-byte float, array size = [polarization_3, look, xdim_grid, ydim_grid]): TA of reflected sun intrusion. Units: Kelvin. polarization basis: 1=I, 2=Q, 3=S3.

- **ta_gal_dir** (4-byte float, array size = [polarization_3, look, xdim_grid, ydim_grid]): TA of direct galaxy intrusion. Units: Kelvin. polarization basis: 1=I, 2=Q, 3=S3.

- **ta_gal_ref** (4-byte float, array size = [polarization_3, look, xdim_grid, ydim_grid]): TA of reflected galaxy intrusion. Units: Kelvin. polarization basis: 1=I, 2=Q, 3=S3.

- **sss_smap** (4-byte float, array size = [look, xdim_grid, ydim_grid]): SMAP sea surface salinity smoothed to approx 70km resolution. Units: PSU. **This is the standard/default product for science applications.**

- **sss_smap_unc** (4-byte float, array size =[look, xdim_grid, ydim_grid]): formal uncertainty estimate of sss_smap. Units: PSU.

- **sss_smap_unc_comp** (4-byte float, array size = [nxdim, nydim, uncertainty_components]): 9 components of formal uncertainty estimate of sss_smap. Units: PSU. See section 8.

- **sss_smap_40km** (4-byte float, array size = [look, xdim_grid, ydim_grid]): SMAP sea surface salinity at original 40-km resolution. Units: PSU.

- **sss_smap_40km_unc** (4-byte float, array size =[look, xdim_grid, ydim_grid]): formal uncertainty estimate of sss_smap_40km. Units: PSU.

- **sss_smap_40km_unc_comp** (4-byte float, array size = [nxdim, nydim, uncertainty_components]): 9 components of formal uncertainty estimate of sss_smap_40km. Units: PSU. See section 8.

- **tb_consistency** (4-byte float, array size = [look, xdim_grid, ydim_grid]): $\sqrt{\chi^2} = \sqrt{\left[T_{B,sur0} - T_{B,RTM}\left(SSS_{SMAP}\right)\right]_{V-pol}^{\ 2} + \left[T_{B,sur0} - T_{B,RTM}\left(SSS_{SMAP}\right)\right]_{H-pol}^{\ 2}}$ of MLE in salinity retrieval algorithm. Units: Kelvin.

- **iqc_flag** (4-byte integer, array size = [look, xdim_grid, ydim_grid]): 32-bit quality control flag (Section 6).

- **sss_ref** (4-byte float, array size = [xdim_grid, ydim_grid]): ancillary reference sea surface salinity from HYCOM. Units: PSU.

- **ta_ant_exp** (4-byte float, array size = [polarization_4, look, xdim_grid, ydim_grid]): expected antenna temperature before any losses. This value is to be compared with **ta_ant_calibrated**. The RTM computation is performed at boresight and based on the HYCOM reference salinity. Units: Kelvin. polarization basis: 1=V, 2=H, 3=S3, 4=S4.

- **tb_sur0_exp** (4-byte float, array size = [polarization_4, look, xdim_grid, ydim_grid]): expected flat surface brightness temperature and **after adding the sea-ice correction term dtb_sea_ice_correction** (section 5.3). This value is to be compared with **tb_sur0**. The RTM computation is performed at boresight and based on the HYCOM reference salinity. Units: Kelvin. polarization basis: 1=V, 2=H, 3=S3, 4=S4.

- **pratot_exp** (4-byte float, array size = [look, xdim_grid, ydim_grid]): expected total polarization rotation angle = geometric part + Faraday rotation. The computation of the Faraday rotation part is based on the ancillary TEC fields from UBern. range: [-90^o, +90^o].

- **TEC** (4-byte float, array size = [look, xdim_grid, ydim_grid]): Vertically integrated electron content between surface and S/C. See section 3.3. The TEC is not used in the salinity retrieval algorithm. It is provided as diagnostic information for tracking the calibration of the 3rd Stokes.

- **anc_sea_ice_flag** (byte, array size = [iceflag_components, xdim_grid, ydim_grid]): ancillary sea-ice detection indicator. A value 1 means that the sea=ice indicator is set. Component 1 = climatological sea-ice mask including iceberg alley near Antarctica. Component 2 = 8-day aggregate sea-ice flag from RSS ASMR-2 AS-ECV V8.2. The aggregate sea-ice flag is set if at least 1 observation within the 8-day period is flagged. Component 3= 8-day aggregate sea-ice flag from Meissner and Manaster (2021).

- **sea_ice_zones** (byte, array size = [xdim_grid, ydim_grid]): sea-ice zones from Meissner and Manaster (2021). See section 5.3.

13.2 Level 3

13.2.1 Paths and Filenames

1. 8-day running averages

- **Pathname***: https://data.remss.com/smap/SSS/V06.0/FINAL/L3/8day_running/yyyy/*

- **Filename:** *RSS_smap_SSS_L3_8day_running_yyyy_doy_FNL_v06.0.nc*
yyyy = 4-digit year, doy= 3-digit day of year.

2. Monthly Averages

- **Pathname** https://data.remss.com/smap/SSS/V06.0/FINAL/L3*/monthly/yyyy/*

- **Filename:** *RSS_smap_SSS_L3_monthly_yyyy_mm_FNL_v06.0.nc*
yyyy = 4-digit year, mm= 2-digit month of year.

13.2.2 Global Attributes

- **first_orbit** (4-byte integer): the 1st rev that is used in the L3 time averaging.

- **last_orbit** (4-byte integer): the last rev that is used in the L3 time averaging.

- **start_time_of_product_interval** (8-byte real): seconds of start time of product interval since 2000-01-01 00:00:00 UTC.

- **end_time_of_product_interval** (8-byte real): seconds of end time of product interval since 2000-01-01 00:00:00 UTC.

13.2.3 Grid and Dimensions

All L3 files are provided on a uniform 0.25°x0.25° rectangular Earth grid.

- The **longitude** varies between 0° and 360° in **nxdim = 1440** uniform 0.25° increments. The longitudinal interval midpoints are: 0.125°, 0.375°, …359.875.

- The **latitude** varies between -90° and +90° in **nydim = 720** uniform 0.25° increments. The latitudinal interval midpoints are: -89.875°, -89.8625°, …, +89.875°.

- The **time** corresponds to the center of the product time interval.

- **uncertainty_components** = 9 specifies the 9 components that go into the formal uncertainty estimate. See section 8.

- **iceflag_components** = 3 specifies the 3 components of the ancillary sea-ice indicator. Component 1 = climatological sea-ice mask including iceberg alley near Antarctica. Component 2 = 8-day aggregate sea-ice flag from RSS ASMR-2 AS-ECV V8.2. Component 3= 8-day aggregate sea-ice flag from Meissner and Manaster (2021).

13.2.4 Variables

- **nobs** (4-byte integer, array size = [nxdim, nydim]): number of smoothed 70-km L2C observations that are averaged into L3 grid cell.

- **nobs_40km** (4-byte integer, array size = [nxdim, nydim]): number of 40-km L2C observations that are averaged into L3 grid cell.

- **sss_smap** (4-byte float, array size = [nxdim, nydim]): SMAP sea surface salinity smoothed to approx 70-km. Units: PSU. **This is the standard/default product for science applications.**

- **sss_smap_unc** (4-byte float, array size = [nxdim, nydim]): formal uncertainty estimate of sss_smap. Units: PSU.

- **sss_smap_unc_comp** (4-byte float, array size = [nxdim, nydim, uncertainty_components]): 9 components of formal uncertainty estimate of sss_smap. Units: PSU. See section 8.

- **sss_smap_RF** (4-byte float, array size = [nxdim, nydim]): rain filtered SMAP sea surface salinity smoothed to approx 70-km. Units: PSU.

- **sss_smap_RF_unc** (4-byte float, array size = [nxdim, nydim]): formal uncertainty estimate of sss_smap. Units: PSU.

- **sss_smap_40km** (4-byte float, array size = [nxdim, nydim]): SMAP sea surface salinity at original 40-km resolution. Units: PSU.

- **sss_smap_40km_unc** (4-byte float, array size = [nxdim, nydim]): formal uncertainty estimate of sss_smap_40km. Units: PSU.

- **sss_smap_40km_unc_comp** (4-byte float, array size = [nxdim, nydim, uncertainty_components]): 9 components of formal uncertainty estimate of sss_smap_40km. Units: PSU. See section 8.

- **sss_ref** (4-byte float, array size = [nxdim, nydim]): HYCOM reference sea surface salinity. Units: PSU.

- **gland** (4-byte float, array size = [nxdim, nydim]): average land fraction weighted by antenna gain. range: [0.0, 1.0].

- **fland** (4-byte float, array size = [nxdim, nydim]):average land fraction within 3-dB contour. range: [0.0, 1.0].

- **gice_est** (4-byte float, array size = [nxdim, nydim]): estimated average sea ice fraction weighted by antenna gain pattern. range: [0.0, 1.0]. See section 5.3.

- **surtep** (4-byte float, array size = [nxdim, nydim]): ancillary sea surface temperature from CMC averaged over L3 time period (8-day, monthly). Units: Kelvin.

- **winspd** (4-byte float, array size = [nxdim, nydim]): ancillary sea surface wind speed from CCMP averaged over L3 time period (8-day, monthly). See Section 4.2.1. Units: m/s.

- **anc_sea_ice_flag** (byte, array size = [iceflag_components, nxdim, nydim]): ancillary sea-ice detection indicator at center day of 8-day L3 field. A value 1 means that the sea=ice indicator is set. Component 1 = climatological sea-ice mask including iceberg alley near Antarctica. Component 2 = 8-day aggregate sea-ice flag from RSS ASMR-2 AS-ECV V8.2. Component 3= 8-day aggregate sea-ice flag from Meissner and Manaster (2021). This variable is provided for the 8-day L3 data.

- **sea_ice_zones** (byte, array size = [nxdim, nydim]): sea-ice zones from Meissner and Manaster (2021) at center day of 8-day L3 field. See section 5.3. This variable is provided for the 8-day L3 data.

13.3 Level 2C NRT

13.3.1 Paths and Filenames

- **Pathname:** https://data.remss.com/smap/SSS/V06.0/NRT/L2C//*yyyy/mm/*...
yyyy = 4-digit year, mm = 2-digit month.

- **Filename:** *RSS_SMAP_SSS_L2C_rnnnnn_yyyymmddThhmiss_yyyyddd_NRT_V06.0.nc*.
nnnnn = 5-digit orbit (rev) #, yyyy = 4-digit year, mm = 2-digit month, dd = 2-digit day of month, hh=2-digit hour of day (UTC), mi = 2-digit minute of hour (UTC), ss = 2-digit second of minute (UTC), doy 3-digit day of year. The time stamp refers to the start time of the orbit.

13.3.2 Global Attributes

Same as in 13.1.2.

13.3.3 Gridding and Dimensions

Same as in 13.1.3.

13.3.4 Variables

Same as in 13.1.4.

APPENDIX A: BACKUS-GILBERT (BG) OPTIMUM INTERPOLATION (OI)

The Backus-Gilbert (BG) Optimum Interpolation is an established and widely used method for sampling and gridding passive microwave satellite data (Poe 1990). It finds a set of weights A_i in the neighborhood of a chosen synthetic target footprint and computes the antenna temperature TA of the target $T_{A,rsp}$ as weighted sum of the individual observations $T_{A,i}$:

$$T_{A,rsp} = \sum_i A_i \cdot T_{A,i} \tag{14}$$

The weights A_i are determined by minimizing the least square deviation of the fit:

$$Q = \iint dxdy \left[G_T(x,y) - \sum_i A_i \cdot G_i(x,y) \right]^2 \tag{15}$$

between the chosen target response (gain) GT and the resampled gain. The index *i* runs over all samples in the neighborhood of the target cell that have a sufficiently large weight A_i to be included in the average (14). In our case we include all samples within a 125 km radius of the target cell.

Carrying out this optimization requires the computation of the normalization integral

$$u_i = \iint dxdy \cdot G_i(x,y) \tag{16}$$

and the two overlap integrals

$$\begin{aligned} v_i &= \iint dxdy\, G_T(x,y) \cdot G_i(x,y) \\ g_{ij} &= \iint dxdy\, G_i(x,y) \cdot G_j(x,y) + \beta \cdot \delta_{ij} \end{aligned} \tag{17}$$

The gain functions G_i of the individual SMAP observations are given by the pre-launch measured patterns of the SMAP antenna and are the individual SMAP gain patterns of the effective field of view (EFOV) 39 x 47 km SMAP TA that are recorded in the L1B files (Piepmeier et al. 2023).

The result of the optimization can be summarized as follows (using vector/matrix notation, the superscript T denotes the transposed vector):

$$\mathbf{A} = \mathbf{g}^{-1} \bullet \left[\mathbf{v} + \frac{\left(1 - \mathbf{u}^{\mathbf{T}} \bullet \mathbf{g}^{-1} \bullet \mathbf{v}\right)}{\mathbf{u}^{\mathbf{T}} \bullet \mathbf{g}^{-1} \bullet \mathbf{u}} \mathbf{u} \right] \tag{18}$$

The parameter β is a small smoothing parameter. Its value is chosen to optimize the noise reduction factor $NRF = \sum_i A_i^2$ compared to the original gain pattern $g_i(x,y)$ in a tradeoff for

the quality of fit Q. A smaller/larger value for β results in a better/worse fit value Q and in a worse/better NRF.

The values of the resampling weights A_i, the fit Q and the NRF depend all on the scanning geometry and the scan azimuth angle.

The target cells for the NASA/RSS SMAP SSS Version 3/4/5 releases are centered on the midpoints of a fixed 0.25° Earth grid whose vertices are located at 0°, 0.25°, 0.5°, … longitude and at 0°, +/- 0.25°, +/-0.5°, … latitude. The target gain patterns g_i are the same as the original 39 x 47 km EFOV footprints. For the smoothing factor β a value of 0.5 is chosen. This results in an average NRF of about 0.4.

The BG OI that is applied in the SMAP L2A processing of the salinity retrieval algorithm is actually done in two steps. The first step in the resampling is to take a single scan and adjust the position of the observations to correspond to integer azimuth angles (i.e., 0° to 359°). The sampling in the along-scan direction well exceeds Nyquist sampling, and therefore the fit accuracy of the resampled data is very high. The second step is the resampling onto the fixed 0.25° Earth grid.